urban science

MDPI

Article

Small-Scale Microclimatic Temperature Variability Shapes Spring Green-Up of Cool- and Warm-Season Turfgrasses

Jose Marin [1], Pedro V. Mauri [2], María del Pilar Garcia de Paredes [3], Ana Centeno [3] and Lorena Parra [3,*]

[1] ÁreaVerde MG Projects S.L., C/Oña 43, Bajo, 28050 Madrid, Spain; jmarin@areaverde.es
[2] Instituto Madrileño de Investigación y Desarrollo Rural, Agrario y Alimentario (IMIDRA), Finca El Encín, Autovía A-2, Km 38,200, 28805 Alcalá de Henares, Spain; pedro.mauri@madrid.org
[3] Departamento de Producción Agraria, Escuela Técnica Superior de Ingeniería Agronómica, Alimentaria y de Biosistemas, Universidad Politécnica de Madrid, 28040 Madrid, Spain; m.garciadeparedes@alumnos.upm.es (M.d.P.G.d.P.); ana.centeno@upm.es (A.C.)
* Correspondence: lorena.parra@upm.es

Abstract

In recent years, the use of warm-season species, which are species requiring less water, has been pursued in continental areas, but their dormancy and spring green-up need to be properly defined. In urban green areas, we find that small-scale microclimatic differences, while less intense than classical urban–rural gradients, still influence vegetation performance and spring green-up. This study examines the impact of microclimatic temperature variation on the spring green-up of different cool-season and warm-season turfgrasses in the continental climate of Madrid, Spain. The evaluation of colour change during the spring green-up process has been conducted using different vegetation indices, and mathematical models for correlating temperature with the indices' values have been obtained. The results indicate that with average temperatures varying by about 1.3 °C and 0.9 °C in January and February, respectively, there have been marked differences in spring green-up, especially in cool-season turfgrasses, of almost one month. In contrast, differences in warm-season turfgrasses were reduced. Among the four vegetation indices, Canopeo has proved to be the best for detecting the early stages of spring green-up, with R^2 values ranging from 0.43 to 0.92. Meanwhile, the tailored greenness index for turfgrass was the most effective for determining the moment at which warm-season grasses achieve the colouration of cool-season grasses, with R^2 ranging from 0.79 to 0.85. Finally, the green leaf index was particularly valuable for identifying differences among species and sectors throughout the entire spring green-up process. Models based on this index achieve high R^2 values (0.57 to 0.94), but these models predict the moment at which warm-season grasses achieve cool-season grasses' colouration later than it actually occurs. Understanding how turfgrasses respond to these localised microclimatic conditions is essential for selecting resilient species and improving maintenance strategies in parks, sports areas, and other components of urban green infrastructure.

Keywords: cool-season turfgrasses; warm-season turfgrasses; mathematical model; vegetation index; GLI; Canopeo; green infrastructure

Check for updates

Received: 27 March 2026
Revised: 12 May 2026
Accepted: 24 May 2026
Published: 2 June 2026

Copyright: © 2026 by the authors. Licensee MDPI, Basel, Switzerland. This article is an open access article distributed under the terms and conditions of the Creative Commons Attribution (CC BY) license.

1. Introduction

Turfgrass is one of the most common surfaces in urban green areas. It provides not only aesthetic value, which can be achieved with artificial turf, but also environmental services, such as carbon sequestration and temperature decrease [1,2]. Compared with

more natural alternatives such as native prairies, turfgrass has a greater potential to reduce water runoff. Additionally, it is an irreplaceable surface for recreational sports and outdoor activities [3,4]. Nevertheless, it requires a high amount of water input for these benefits to be provided [2,4], and its periodic mowing requires fuel consumption and labour, making turf maintenance more expensive than other green infrastructure typologies [5]. Furthermore, climate change is leading to fluctuations in temperature and precipitation that will result in a greater need to save water in the management of turfgrasses [6]. Moreover, urban small-scale microclimatic thermal differences can clearly affect phenological development and plant requirements in green areas. In this scenario, the selection of more water-efficient species is one possible solution [7].

Turfgrass species can be classified according to their photosynthetic pathway during the cool season, as C3, and the warm season, as C4. C4 species present different leaf hydraulics, with rapid stomatal closure that allows for a reduced loss of water during transpiration, making them more water-efficient [8–10] and more tolerant towards irrigation deficit [11]. C4 species thrive at higher temperatures than C3 species, which means they are adapted to warm environments with mild winters [12]. Additionally, spring green-up differs between species groups, typically occurring earlier in C3 than C4 species, and local temperature variations may delay or advance this process. During cold winters, C4 species enter dormancy and lose their pigmentation [13]. Once the temperature starts increasing, C4 species initiate their spring green-up processes, which differ among species. As a result, cool-season species are widely used at present [14]. Nonetheless, considering that winters are becoming milder in southern European regions [15,16], the dormancy period for warm-season turfgrasses in these places might decrease in the future [17]. In order to predict when and how future lawns might react to this advantage, the relationship between the end of spring green-up or the greenness of turfgrass and temperature must be modelled. Apart from global temperature changes, microclimatic variations due to surrounding architecture, particularly important in urban green areas, must be taken into account. Together, these factors highlight the complexity of spring green-up dynamics, particularly in urban environments, which are being influenced by both climate trends and small-scale microclimatic conditions. Although some studies have observed that tree species exhibit earlier green-up and flowering near urban areas [18,19], the combined effect of small-scale microclimatic conditions and species-specific responses on turfgrass spring green-up remains poorly understood.

To monitor plant behaviour and the visual aspect of the turfgrass, vegetation indices are useful, objective tools for measuring aesthetic value. The use of spectrophotometry can go as far as showing differences between turf cultivars within the same species [20]. The Normalised Difference Vegetation Index (NDVI), Green Area, Greener Area, and RGB vegetation indexes are used to determine turfgrass behaviour under water-stress conditions [21–23]. The NDVI can also be used to assess visual quality [22,23]. Other indices that have been used to measure water and nutrient stress are the Water Band Index (WBI), simple Ratio Vegetation Index (RVI) or Green-to-red Ratio Index (GRI) [24]. Among these indices, those relying on RGB data are the easiest to use due to the absence of specialised equipment.

The environmental conditions that affect spring green-up represent a vast area of study across different species. Increased precipitation in a semi-arid climate might have a stronger effect too [25]. Higher temperatures result in earlier green-up dates [26]. Yet it has been observed that, in warmer climates, photoperiod control has a bigger impact on the hastening of spring green-up date than temperature [17]. Regarding turf management, De Luca & Gómez de Barreda [27] measured, using the NDVI and the green area percentage, the effect of an amino acid-based biostimulant on hastening spring green-up. Çakir

et al. [28] measured shoot density using a visual scale and manual counting, and found that nitrogen application maintains green coverage of zoysia grass during winter and fall in a subtropical climate. Latitude is also a factor to consider. Fu et al. [29] observed a mean difference of 47 days per degree of latitude required for spring green-up between 35° N and 70° N in Eurasian grasslands. Magni et al. [30] studied different varieties of *C. dactylon* at two locations with different latitudes in Italy and found that species at lower latitudes had earlier spring green-up.

In urban areas, the most studied microclimatic temperature differences are those associated with the Urban Heat Island (UHI). The UHI is part of the rural–urban differences and can be considered a high-scale microclimatic effect [31]. Several authors have pointed out the impact of vegetation canopy on reducing the severity of the UHI [32,33]. Moreover, Zipper et al. [34] demonstrated the effect of the UHI on advancing plant phenology and the growing season by up to 5 days in Madison. In their study, they used remote sensing data, including different ground covers across different tree and grass species, and HOBO U23 Pro v2 temperature/RH sensors. The authors differentiated three regions in the study: rural, park, and urban. Meanwhile, Meng et al. [35] studied the advancement of the start of the season due to temperature along 85 large rivers in the United States. The authors identified the impact of the UHI on advancing the start of the season by 6 days in cities compared to rural areas. The authors used remote sensing data, and their results are not focused on the impact of the UI on a particular species.

Nevertheless, intra-urban temperature differences, also known as small-scale microclimatic effects, are another important difference and are less reported. Recent studies demonstrated intra-urban microclimatic differences ranging from −1.1 to 1.3 °C [36]. These small-scale differences are often caused by local factors such as radiation exposure, surrounding structures, surrounding materials, vegetation configuration, and wind sheltering, among others. These differences can have a considerable impact on green areas and should be considered in their design and maintenance. The effect of small-scale differences on plant phenology is less studied, as the approaches used in UHI studies on plant phenology, mainly relying on remote sensing data [37], are not applicable at this scale. Moreover, even in UHI studies, the use of remote sensing data prevents a detailed study of this impact in a particular species, such as turfgrass. For these studies, proximal sensing is required as an on-site monitoring technology for temperature data acquisition. As far as we are concerned, the effect of small-scale microclimatic temperature differences—therefore allowing temperature effects to be isolated from photoperiod—has not been explicitly addressed for turfgrass spring green-up in continental regions.

The aim of this paper is to assess the impact of small-scale microclimatic thermal differences on the spring green-up of different turfgrass species. Here, microclimatic temperature differences refer to horizontal, small-scale thermal variability, caused by local exposure and sheltering conditions, rather than vertical gradients or regional urban–rural temperature contrasts. These microclimatic horizontal differences have been studied in a region of the peri-urban area of Madrid. Spring green-up will be evaluated using different vegetation indices derived from RGB data. Accumulated temperature in the three microclimatic zones is measured with deployed temperature sensors. Data from vegetation indices are statistically analysed, and models for predicting the end of spring green-up are compared. The main contribution of this paper is to determine the thermal accumulation at which each warm-season species reached greenness values comparable to those of cool-season species. Moreover, this paper examines the selection of the most suitable vegetation index to assess turfgrass greenness. Therefore, the present study is primarily framed within the field of urban climate science, focusing on small-scale microclimatic thermal variability

within urban green spaces and its functional implications for managed vegetation relevant to urban green area management.

2. Materials and Methods

2.1. Location Description

The tests were conducted in the experimental fields of the Escuela Técnica Superior de Ingeniería Agronómica, Alimentaria y de Biosistemas from the Universidad Politécnica de Madrid. These experimental fields are located in the western part of Madrid. Besides the climate, this location is characterised by its proximity to the Manzanares River and to one of Madrid's main roads, which provide a typical peri-urban environment. The soil characteristics, as shown in Table 1, indicate that the soil is a loamy sand, comprising approximately 74% sand, 18.6% silt, and 7.2% clay. These percentages ensure excellent drainage properties and indicate the need for relatively high-frequency irrigation. The soil is slightly alkaline with a pH of 7.54 and a low electrical conductivity of 113 µS/cm, both of which support optimal turfgrass development. Regarding the nutrient levels, the obtained values show moderate concentrations of sodium (85 ppm) and potassium (80 ppm), while calcium is relatively low at 40 ppm. Although the Na+ concentration is relatively high, it does not exceed the range considered healthy for soil. Meanwhile, the content of NO_3^-, 170 ppm, suggests good nitrogen availability for turfgrass growth.

Table 1. Main soil parameters.

Parameter	Value
Na^+ (ppm)	85
K^+ (ppm)	80
Ca^+ (ppm)	40
NO_3^- (ppm)	170
pH	7.54
Conductivity (µS/cm)	113
Clay (%)	7.2
Silt (%)	18.6
Sand (%)	74.2

Regarding the climate, more information will be provided in Section 3 based on the mean local data gathered by on-site sensors. Regardless, some non-temperature-related climatic information from a nearby station is provided to characterise the climate during the studied period. This weather station, located less than 1 km from the studied area, was used solely to characterise background meteorological conditions during the experimental period and was not intended to represent plot-level microclimatic conditions. The region in which the test was conducted is characterised by a Mediterranean climate and is classified as USDA Hardiness Zone 9. The test was carried out during a particularly rainy season. January had 23 cloudy days and 15 rainy days. Meanwhile, February had 16 cloudy days and 5 days of rain, each lasting only a short time. Rain was recorded on more than 21 days in March, with only 4 days without clouds. These clouds remained present in April, with only 5 days of clear sky. Nonetheless, rainfall intensity decreased with precipitation over 15 days. In May, conditions changed, with a few rainy days of short duration and only 18 cloudy days.

Regarding potential advective effects among plots, the area's boundary conditions are homogeneous. Even though this effect cannot be fully excluded, it is considered secondary to a low wall that locally modifies surface airflow by reducing wind speed and, consequently, convective heat transfer in the turfgrass area, thereby driving the observed temperature gradient. This wall is located in the northern part of the plots, providing shel-

ter from the dominant winter wind from the northwest, as shown in Figure 1. Additionally, Figure 1a,b contain other relevant information about the surroundings of the trial, while Figure 1c provides a detailed view of the existing tree canopy and buildings. As can be seen, the experimental plots are located in an open area with a high sky view factor. Surrounding buildings and tree canopy cast a homogenous shade over the plots, with limited shade at the beginning of the morning. Seasonal shading patterns were more pronounced during winter months and progressively diminished towards spring.

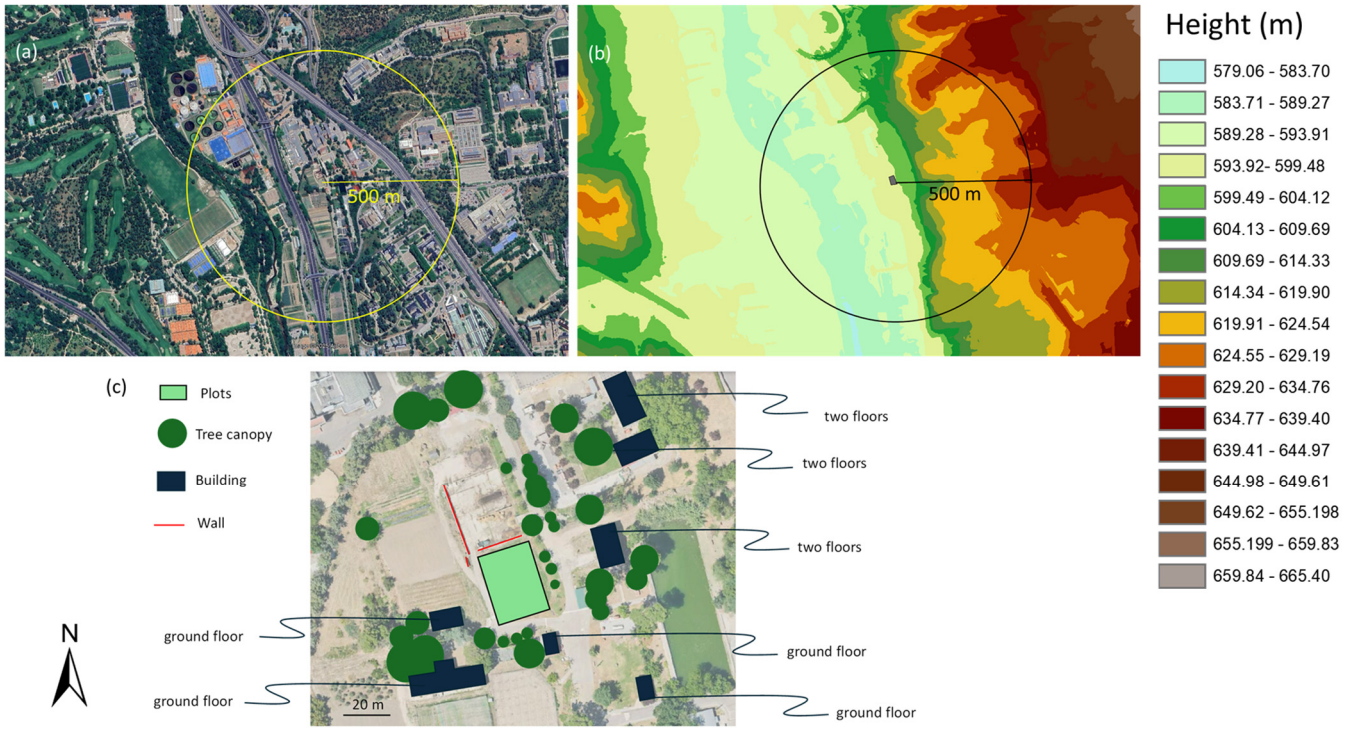


Figure 1. The surroundings of the trial area: (**a**) the orthophotography of the area, (**b**) a terrain elevation model of the area, and (**c**) a detailed map with tree canopy, buildings and walls.

2.2. Plant Material and Experimental Design

The used plant material includes two warm-season, or C4, species, which are compared with cool-season, or C3, grasses. While the C4 species are grown as a monoculture, the C3 grasses are grown as a grass mixture including three different species. A total of two C4 and three C3 species are selected for the test. The species used in the different mixes are shown in Table 2. It should be noted that the selected C3 species are the mix generally used for green areas in Spain.

Table 2. Used species in mixture and monoculture plots.

Class	Species	Cultivar	Percentage
C3 mix	*Festuca arundinacea* Schreb	ESTRENA	60%
	Poa pratensis L.	SAONA	10%
	Lolium perenne L.	CT7	30%
C3/C4 mix	*Cynodon dactylon* × *Cynodon transvaalensis*	Texoma (OKC1876)	100%
	Festuca arundinacea Schreb	ESTRENA	Overseed 40 g/m^2 with 70%
	Lolium perenne L.	CT7	Overseed 40 g/m^2 with 30%
C4 (I)	*Zoysia matrella* Merr.	Zorro	100%
C4 (II)	*Cynodon dactylon* × *Cynodon transvaalensis*	Texoma (OKC1876)	100%

From each of these combinations, 9 plots of 2 × 2 m were established. These 9 plots were distributed in 3 blocks characterised by small microclimatic differences. Each one of the blocks consists of 12 plots. A randomised process determined the exact location of each species. The disposal of turfgrass species along the blocks or sectors can be seen in Figure 2a, as well as their specific location regarding Madrid city (b) and the Iberian Peninsula (c).

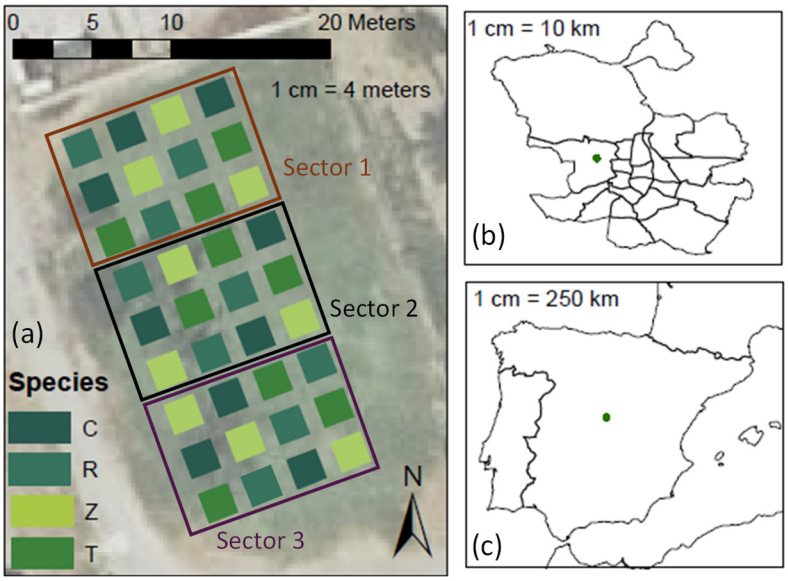


Figure 2. Design of trial (**a**) and its location at municipal (**b**) and national (**c**) scale.

2.3. Evaluation of Microclimatic Differences

To assess the differences between blocks, or sectors, due to microclimatic conditions, sensors were installed in the fields. One temperature sensor (Plantae®, Madrid, Spain) was located in the central plot of each block. The sensors gather data hourly and send them to a web server. The temperature sensor was located at 5 cm from the turfgrass canopy or 10 cm from the soil surface; thus, the measured temperatures correspond to the temperature of the air that surrounds the turfgrass leaves. Contact temperature sensors were used to reduce potential biases associated with radiative effects and micro-shadowing.

Accumulated temperature of the turfgrass was estimated as Growing Degree Days with a base temperature of 0 °C (GDD_0), calculated via Equation (1), where T_{max} is the maximum daily temperature and T_{min} is the minimum daily temperature. We have set $T_{base} = 0$ °C due to the different species included in the models and the absence of a reliable base temperature for the triggering of spring green-up. Negative daily values were set to zero prior to accumulation. Daily GDD_0 values were accumulated from 1 January 2024 until each image acquisition date.

$$GDD_0 = \left(\frac{T_{max} + T_{min}}{2}\right) - T_{base} \quad (1)$$

In addition to continuous block-level temperature monitoring with the aforementioned sensors, occasional measurements of canopy and soil temperatures were collected across plots for calibration. These measurements were conducted from 28 February to 22 May at five different times. Moreover, soil moisture (FieldScout TDR 350, Spectrum Technologies, Inc., Aurora, IL, USA) and NDVI (Greenseeker Handheld, Trimble Inc., Westminster, CO, USA) data were collected at different times throughout the trial.

2.4. Study Period and Image Acquisition Process

The turfgrass was established on 20 November 2024 and was managed equally throughout the entire period in terms of irrigation, fertilisation, and mowing, with the sole differences among blocks being microclimatic conditions. The image acquisition process began on 1 February 2025, the moment at which the first signs of spring green-up were detected in the C3/C4 mix. The process was completed on 20 May 2025, the moment when all plots had finished the spring green-up process, as assessed by the visual quality of the turfgrass in all included plots. The time lapse between images was variable and adjusted to visually observed differences. At the beginning of the process, in February and March, the images were taken every two weeks. Nonetheless, once the spring green-up accelerated due to the climatic conditions, images were captured approximately once a week from April. Images were captured on 13 different days during the experiment, corresponding to Day of the Year (DoY) 31, 45, 59, 73, 87, 94, 101, 112, 118, 125, 132, 139 and 155.

Regarding the image acquisition process, in order to avoid illumination differences and interferences among blocks, pictures were taken of the 12 plots of each block. Three images, one per block, were captured at the same moment with barely any light differences among them. The images were captured with a Xiaomi M2007J3SG digital camera (Xiaomi, Beijing, China). The dimensions of the images were 5760 × 2592 with a bit resolution of 24. The settings were manually adjusted to the following: exposure time of 1/605s, ISO velocity of 50, focal distance of 7 mm, and aperture maximum of 1.51.

The exact point at which images were captured was marked, and the pictures were taken from the same location at a height of 145 to 150 mm during the entire period. Images were gathered approximately at the same hour; nevertheless, light conditions between different days were variable. These differences are particularly important at the beginning of the dataset since there was a long period with continuous cloud coverage from February to April. An example of one of the gathered images can be seen in Figure 3.



Figure 3. Example of gathered image.

2.5. Image Processing and Index Selection

Since each image contains the 12 individual plots, images were manually cropped to obtain 12 subimages from each picture, each containing a single plot. These images were tagged with the ID of each plot. Given the plots' different locations, the individual images vary in size, ranging from 370 × 56 to 492 × 140. A total of 432 subimages were obtained after initial image processing.

After preprocessing, the images were processed using Matlab R2025 software [38]. First, histograms were obtained for each subimage. Then, these histograms were normalised because the total number of pixels differed across subimages. After normalising the previously proposed histograms, the indices described in [39] were applied. These indices use two ranges of the histogram to estimate the greenness and the homogeneity of the turfgrass. The ranges of the histogram were manually adjusted according to the obtained

subimages. The green range was defined as brightness green values from 60 to 154, while the yellow range was set from 160 to 185. With these two ranges, Equations (2) and (3) were applied to obtain the indices:

$$Greeness = \frac{\sum(pixels\ G_{60–154})}{\sum(pixels\ G_{0–255})} \quad (2)$$

$$Homogenity = \frac{\sum(pixels\ G_{60–154}) - \sum(pixels\ G_{160–185})}{\sum(pixels\ G_{60–154}) + \sum(pixels\ G_{160–185})} \quad (3)$$

Meanwhile, two well-known indices were also applied. The selected indices include the Canopeo, obtained according to the equations described in [40], and the Green Leaf Index (GLI) according to the description in [41]. The equation of the GLI can be seen in (4), while the equations for determining whether a pixel is vegetation or not, according to Canopeo, are presented in (5)–(7). Equations (5)–(7) are applied to every pixel, and only if all three equations are true is the pixel considered vegetation. The final metric is the percentage of pixels considered vegetation. Meanwhile, the GLI is calculated for every pixel, and then an average value is provided. While greenness and homogeneity are applied as an index for the entire subimage based on the histogram values, the GLI and Canopeo are applied pixel by pixel.

$$GLI = \frac{2 \times G - B - R}{2 \times G + B + R} \quad (4)$$

$$\frac{R}{G} > 0.95 \quad (5)$$

$$\frac{B}{G} > 0.95 \quad (6)$$

$$2 \times G - R - B > 20 \quad (7)$$

It should be noted that RGB imagery under natural field conditions suggests that variations in illumination (e.g., shadows and changing light conditions) may influence the resulting vegetation indices, as stated in the literature [42]. Although no formal radiometric correction was applied, images were acquired at the same time of day and from the same position under non-extreme weather conditions. Moreover, two of the indices used, the GLI and Canopeo, are robust to moderate changes in illumination and outperform other RGB-based indices [43,44].

2.6. Statistical Information

Once all the values for the indices were obtained, the data were statistically analysed using Stagraphics 18 software [45]. First of all, we evaluated the differences in indices by means of a multifactorial ANOVA. Initially, the ANOVA model was configured with interaction order 1, which in Statgraphics includes only main effects, using as factors mix (C3, C3/C4, C4(I) or C4(II)) and microclimatic zone (or block). Multifactorial ANOVAs were conducted for each date to assess the potential of the used indices to differentiate among turfgrasses from different species and sectors on the same date. Then, the model was adjusted to an interaction order of 2 to include two-way interactions (SP × Sector, SP × Date, Sector × Day of the year (DOY)). In both cases, Least Significant Difference (LSD) was used to find which specific group means differ from others.

After evaluating the indices using multifactorial ANOVAs, regression models were calculated to relate each index to the thermal accumulation, as defined in Section 2.3. Only simple models were used. Indices were calculated for each turfgrass mix. For each index, the same model type (Linear, Exponential, Logarithmic, etc.) was used to maintain consistency across the models obtained for the included turfgrass mixes. Thus, only the a

and b factors vary across the equations obtained for each index. The varied plant physiology of the included species can thus explain the variation in a and b. The obtained models for each index are compared to assess the moment at which the C4 and the C3/C4 mix reach the score of C3 turfgrass or reach its maximum value, indicating the end of spring green-up. Thus, it would be possible to assess the accumulated temperature required by each species to finish the spring green-up process.

3. Results

3.1. Differences in Temperature of Plots over Time

In this subsection, we describe the microclimatic differences in plots over the experiment. In Figure 4, we present the thermal accumulation starting from January. The three zones present differences in accumulated temperature, which vary throughout the study period. During the coldest months, Zone 1 is has the highest temperature. A low wall (about 60 cm high) creates a microclimate by serving as a windbreak, reducing the impact of cold mountain winds. Despite its small height, it creates a sheltered zone that protects low vegetation and mitigates wind chill. Differences between the three zones are minimal.

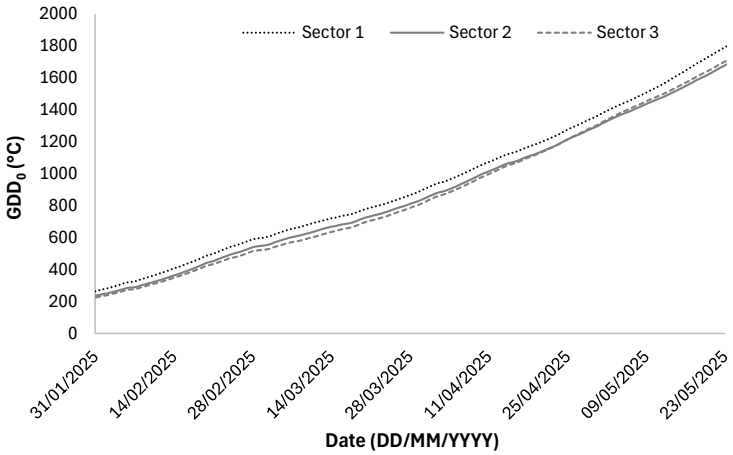


Figure 4. Accumulated temperature as GGD_0 in each sector.

Additionally, Table 3 presents the maximum (Max) and minimum (Min) temperatures recorded in each sector for each month. Moreover, the averaged temperature (Avg), i.e., the mean hourly temperature for each sector and month, is included. Finally, the percentage of time for which each sector was below 5 (% < 5), 0 (% < 0) and −5 (% < −5) °C has been outlined in this table. It is evident that major differences among plots occur in January and February. If we consider Sector 2, the central one, as the reference, the monthly average temperature variation ranged from +0.93 °C to −0.51 °C from January to February, while the maximum daily average temperature variation reached +2 °C to −3 °C. This variation in temperature range falls within the microclimatic variation reported by Kousis et al. [36].

The data collected with handheld devices to measure soil and canopy temperatures were consistent with the continuous monitoring results. Canopy temperatures differed significantly among blocks, with *p*-values ranging from 0.0075 to <0.0001. Temperatures were consistently higher in Sector 1, with canopy temperatures ranging from 2.75 to 3.5 °C above those observed in the coolest sector. Soil temperature measurements confirmed these differences, with *p*-values < 0.0001 and observed temperature differences ranging from 1.2 to 4.7 °C between the warmest and coolest sectors.

Regarding soil moisture measurements, the data indicated significant differences among plots (*p*-values from 0.0017 to 0.0027), with higher soil moisture in Sector 3 and lower values in Sector 1. Nevertheless, the observed differences in soil moisture were

relatively small (ranging from 2% to 4%). These differences may be associated with local microclimatic conditions, including variations in canopy and soil temperatures, which may influence soil water evaporation. Finally, independent NDVI measurements confirmed a significant effect of sector ($p < 0.01$ in all cases), supporting the presence of consistent thermal variability across blocks and its association with spring green-up patterns.

Table 3. Additional climatic information on different sectors.

Month	January	February	March	April	May
			Sector 3		
Avg	3.92	5.62	7.58	13.15	17.32
Min	−11	−7	−5	−1	2
Max	22	27	28	33	41
% < 5	46.6	53	32.3	10.1	2.3
% < 0	21.9	29.5	5.2	0.3	0
% < −5	10.7	3.7	0	0	0
			Sector 2		
Avg	4.43	6.06	7.31	12.34	16.3
Min	−11	−8	−6	−1	1
Max	23	29	27	32	40
% < 5	42.7	52.4	33.9	13.9	3.1
% < 0	21.2	28.9	6.5	0.4	0
% < −5	10	4.3	0.1	0	0
			Sector 1		
Avg	5.28	6.99	7.63	12.76	17.34
Min	−11	−7	−5	−1	3
Max	25	30	27	32	42
% < 5	37.6	49.1	31.9	12.4	0.7
% < 0	19.3	26.2	6.2	0.4	0
% < −5	9.6	2.2	0	0	0

3.2. Differences in Vegetation Indices over Time

In this subsection, we analyse the differences among vegetation indices due to microclimatic differences, species, and period.

3.2.1. Canopeo

Regarding the Canopeo tool, the detailed results of the multifactorial ANOVAs for green canopy coverage are shown in Table A1. Multifactorial ANOVAs were calculated for each date.

The results indicate that it is possible to differentiate among species from the end of January to 12 May, as shown in Figure 5. After that date, although there are some differences among species, the canopy values are too similar, and it is not possible to attribute these observed differences to different species. In general terms, it is possible to affirm that T is the mixture characterised by a higher canopy value. After 11 April, C has canopy values similar to T, being classified in the same group according to the multifactorial ANOVA from 11 April to 12 May. After that period, there are no differences among species.

Regarding the applicability of this index for differentiating among microclimatic zones, the results indicate that differences are significant only during late spring green-up, primarily due to an abnormally high value in S3. The differences among microclimatic zones beyond statistical significance are shown in Figure 6. It is evident that at the beginning of the period (February), canopy coverage is minimal for S1 and maximal for S3. Nonetheless,

this trend is reversed from March to the middle of May, and in the last data collection round, S1 again shows the lowest values.

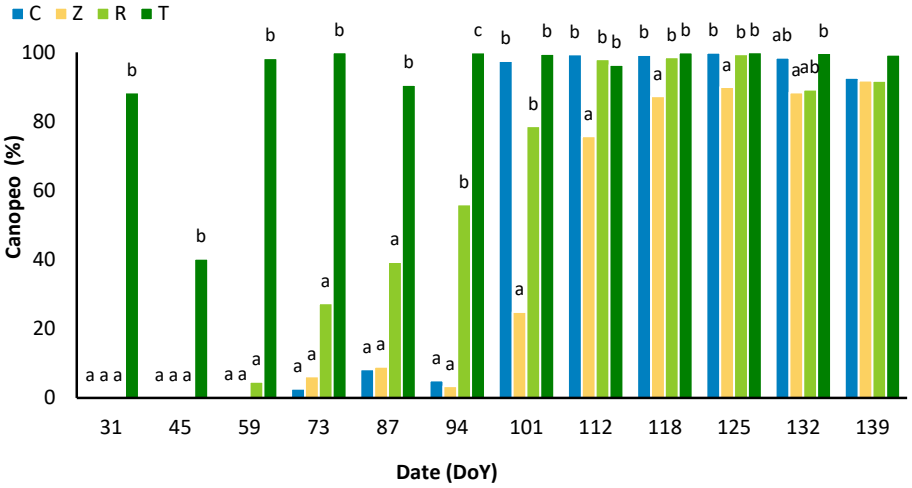


Figure 5. Average values and assigned groups among different species for multifactorial ANOVA for different dates using green canopy coverage tool. Different lowercase letters indicate significant differences (LSD test, $p < 0.05$).

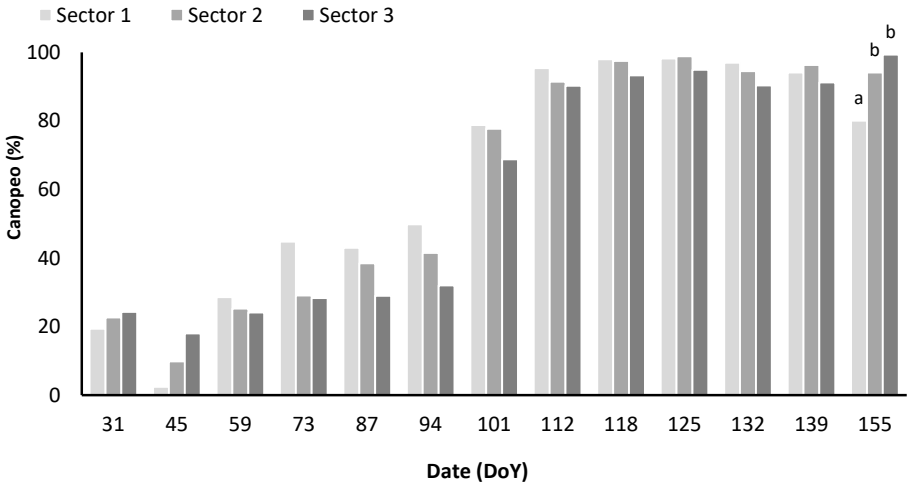


Figure 6. Average values and assigned groups among different sectors for multifactorial ANOVA for different dates using green canopy coverage tool. Different lowercase letters indicate significant differences (LSD test, $p < 0.05$).

A major problem with the canopy coverage index is caused by the saturation of the canopy when it approaches 100%, which prevents the identification of differences. Thus, canopy coverage is an inadequate indicator for turfgrass evaluation because it saturates at 100%, preventing the detection of further physiological or visual enhancements beyond complete cover. Nevertheless, it might be a good indicator for the preliminary stages of turfgrass spring green-up. It must be stated that even though a grass surface reaches 100% canopy coverage, this aspect is not optimal. This is due to the canopy index not being able to assess the intensity of canopy greenness, which is important for the aesthetic value of turfgrass.

3.2.2. Greenness

Regarding the values obtained with the previously proposed greenness index, which only uses the green histogram, the detailed results of the multifactorial ANOVAs are presented in Table A2. Again, multifactorial ANOVAs were calculated for each date.

For the previously proposed index, the results indicate that it has been possible to differentiate among species at different dates, but with an inconsistent pattern, as shown in Figure 7. There are some dates on which the index is unable to differentiate among species due to varying solar exposure and the presence of shadows in the included pictures. It is worth mentioning that for this index, T is the species with the highest value on all dates, which reflects the reality of the observed performance of grasses. Differences between C and Z vary throughout spring green-up according to this index. On 28 April and 12 May, the values for this index for C and T show no statistically significant differences and are similar. Meanwhile, differences between T and Z are even smaller.

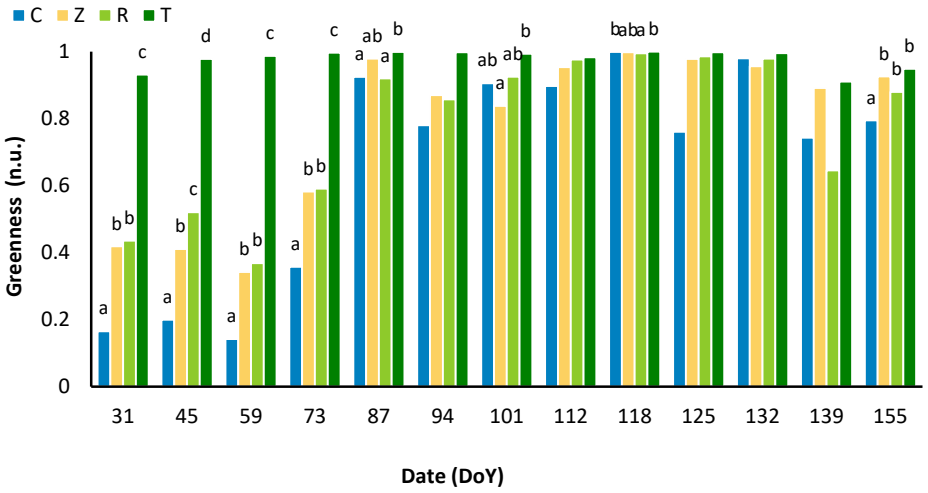


Figure 7. Average values and assigned groups among different species for multifactorial ANOVA for different dates using adapted greenness index. Different lowercase letters indicate significant differences (LSD test, $p < 0.05$).

Regarding the applicability of this index for differentiating among microclimatic zones, the results indicate that differences are significant only at two points during spring green-up, with lower greenness in S3. Regarding the differences among microclimatic zones beyond statistical significance, it is possible to see that at the beginning (during February, March, and part of April), greenness is maximum for S1 or S2 and minimum for S3. After that period, the differences are not stable and vary among dates, as shown in Figure 8.

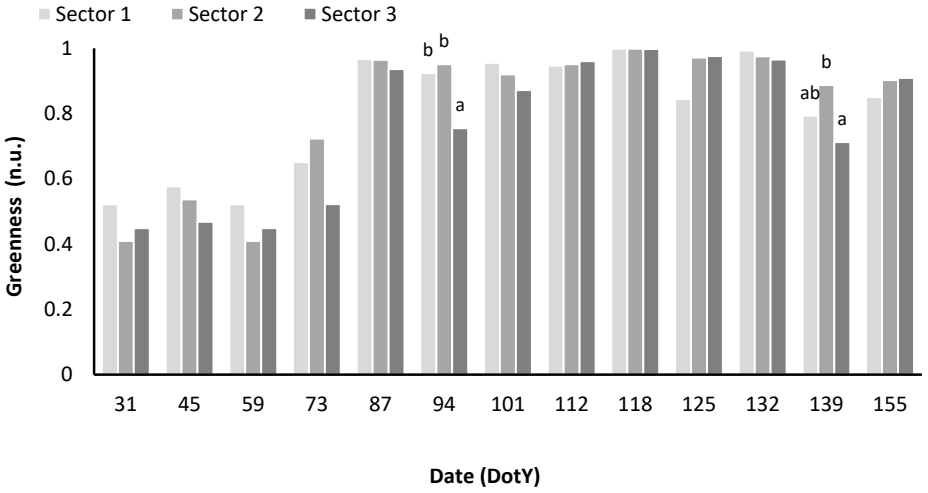


Figure 8. Average values and assigned groups among different sectors for multifactorial ANOVA for different dates using adapted greenness index. Different lowercase letters indicate significant differences (LSD test, $p < 0.05$).

The main drawback of this index is that, because it operates on a single band, it cannot compensate for the effects of shadows in images. Moreover, the defined portion of the histogram for greenness has been modified to include the darkest colourations observed during late spring green-up. This index can be useful for evaluating the spring green-up process under controlled, no-shadow conditions.

3.2.3. Homogeneity

Following this, we describe the results from multifactorial ANOVAs, along with the homogeneity index values (see Table A3). These values are also compared with those obtained using the previously proposed greenness index. As in the previous cases, multifactorial ANOVAs were calculated for each date.

For the adapted homogeneity index, the results indicate that it is possible to differentiate among species mainly at the beginning and at the end of spring green-up, as shown in Figure 9. As for the greenness index, T is the species with the highest value across all dates. Meanwhile, C is the species that starts with a lower homogeneity value and takes more time to increase its value. By the end of March, the homogeneity index of C is similar to that of the rest of the species, and differences among species are not statistically significant. In general terms, we can affirm that C has the lowest values of homogeneity even during summer. This can be explained by differences in colouration of this species, rather than delayed spring green-up. Meanwhile, the differences between Z and T after 22 March are barely insignificant, less than 3% on average.

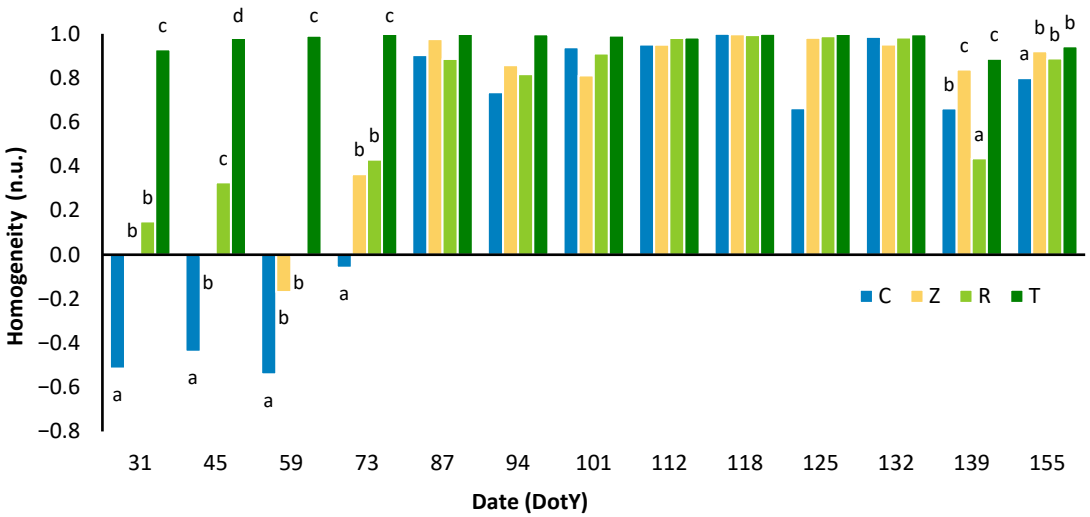


Figure 9. Average values and assigned groups among different species for multifactorial ANOVA for different dates using adapted homogeneity index. Different lowercase letters indicate significant differences (LSD test, $p < 0.05$).

Regarding the application of this index to differentiate among the microclimatic zones, the results indicate that differences are significant only in three moments of the spring green-up, with the lowest homogeneity in S3 (see Figure 10). In this case, the lowest values for S3 along the period are only clearly visible on some dates. This suggests that this index is not sufficiently useful for differentiating among microclimatic zones.

The main problems with this index are that it only uses a single band, and even though it has been specially designed for turfgrass, the effect of shadows strongly affects the performance of this index, as can be seen for Date 12. As stated for the greenness index, the homogeneity index can help evaluate spring green-up processes under controlled light conditions.

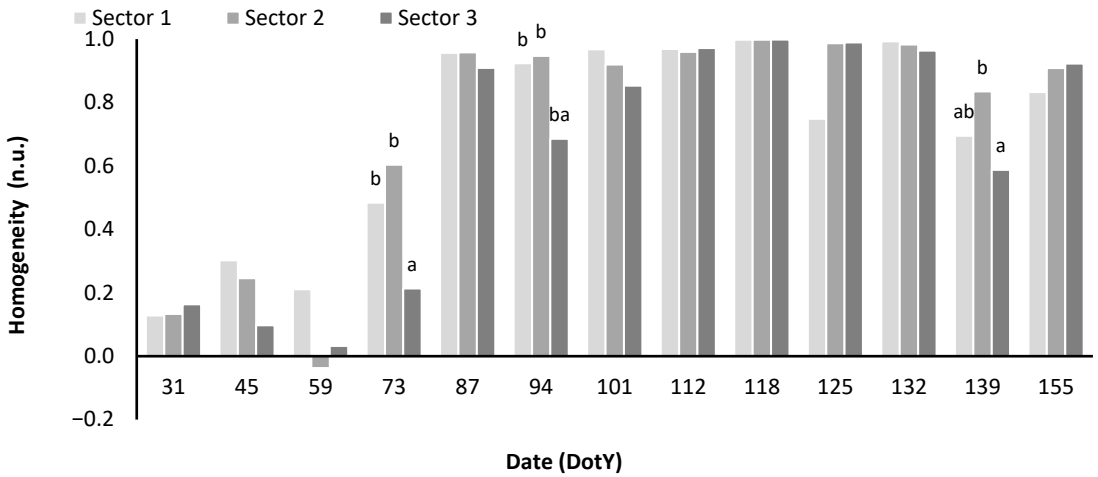


Figure 10. Average values and assigned groups among different sectors for multifactorial ANOVA for different dates using adapted homogeneity index. Different lowercase letters indicate significant differences (LSD test, $p < 0.05$).

3.2.4. GLI

Regarding the values obtained with the GLI, the detailed results of the multifactorial ANOVAs can be seen in Table A4. Again, multifactorial ANOVAs were calculated for each date.

The results indicate that it is possible to differentiate among species over the studied period, as shown in Figure 11. For the obtained GLI values, T is the mixture characterised by the highest performance across almost all dates. Only on the last date, 05 June, does Z outperform T in terms of GLI values, and it is even classified as a different group. According to the GLI results, Z took more time to start the spring green-up process than C. Nonetheless, after 11 April, the values of Z are better than those for C. Thus, comparing the results with the other indexes, this index seems to be the most efficient in differentiating between species during spring green-up and it might be even be capable to differentiating between them during summer, which indicates that this is a promising index for turfgrass colour assessment.

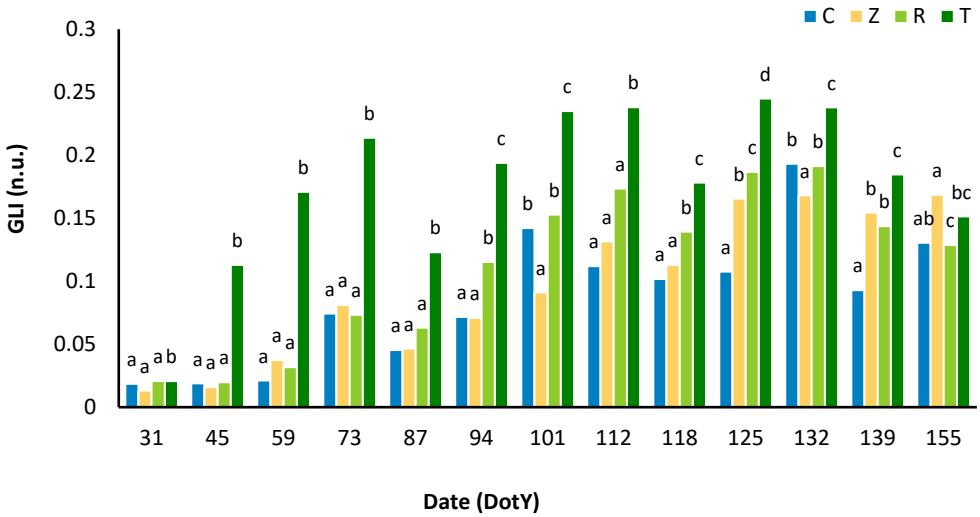


Figure 11. Average values and assigned groups among different species for multifactorial ANOVA for different dates using GLI index. Different lowercase letters indicate significant differences (LSD test, $p < 0.05$).

Regarding the potential application of the GLI to differentiate among microclimatic zones, the results indicate that this index can identify differences during middle and late spring green-up, as shown in Figure 12. In early to mid-spring, when differences are statistically significant, S3 has the lowest value, while S1 shows the highest performance. Nevertheless, for late spring green-up, this trend is reversed, with S3 showing the highest values and S1 the lowest.

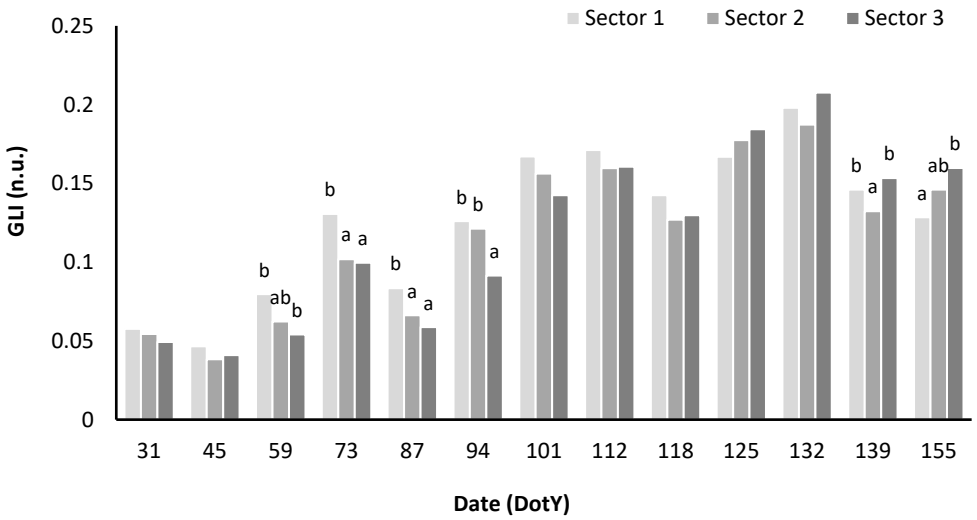


Figure 12. Average values and assigned groups among different sectors for multifactorial ANOVA for different dates using GLI index. Different lowercase letters indicate significant differences (LSD test, $p < 0.05$).

This index has been demonstrated to be a powerful tool for evaluating not only differences among species but also among microclimatic zones. Moreover, the effects of shadows in images for Date 12 are not clear, since the values of the index for this date are consistent with those of the previous and subsequent data. Thus, this index should be explored in the future as a potential, automatic, and objective option for evaluating colour and appearance among turfgrass species. Given the limited effect of shadows on the results, this index can be used without requiring a lightbox to ensure stable light conditions.

3.2.5. Two-Way ANOVA

Finally, as a comparison among the different indices, two-way ANOVAs were conducted with each of the indices as factors, including DOY, species/mixture, and sector/block, as well as their interactions. A summary of these analyses is presented in Table 4. The results indicate that, for all indices, all factors are significant, and almost all interactions are significant, except DOY with sector for Canopeo. The greenness and GLI data have the lowest *p*-values for all factors. This information aligns with the results presented in previous sections.

Table 4. Summary of *p*-values from two-way ANOVA for each index.

Factor/Interaction	Canopeo	Greenness	Homogeneity	GLI
DoY	0.0000	0.0000	0.0000	0.0000
SP	0.0000	0.0000	0.0000	0.0000
Sector	0.0130	0.0000	0.0003	0.0000
DoY × SP	0.0000	0.0000	0.0000	0.0000
DoY × Sector	0.2297	0.0000	0.0001	0.0001
SP × Sector	0.0000	0.0003	0.0021	0.0000

3.3. Obtained Regression Models

In this subsection, we analyse the differences among vegetation indices in the obtained regression models to evaluate spring green-up in relation to thermal accumulation. Given the trend reversal observed on the last day, these data will not be included in the models.

3.3.1. Canopeo

The obtained mathematical models that correlate the accumulated temperature with the Canopeo index can be seen in Figure 13. These models follow a Double Square Root equation in all cases, as shown in Equation (8). The obtained coefficients for the models, along with their correlation coefficients, R^2, and *p*-values, are presented in Table 5.

$$Canopeo = \left(a + b \times \sqrt{GDD_0}\right)^2 \quad (8)$$

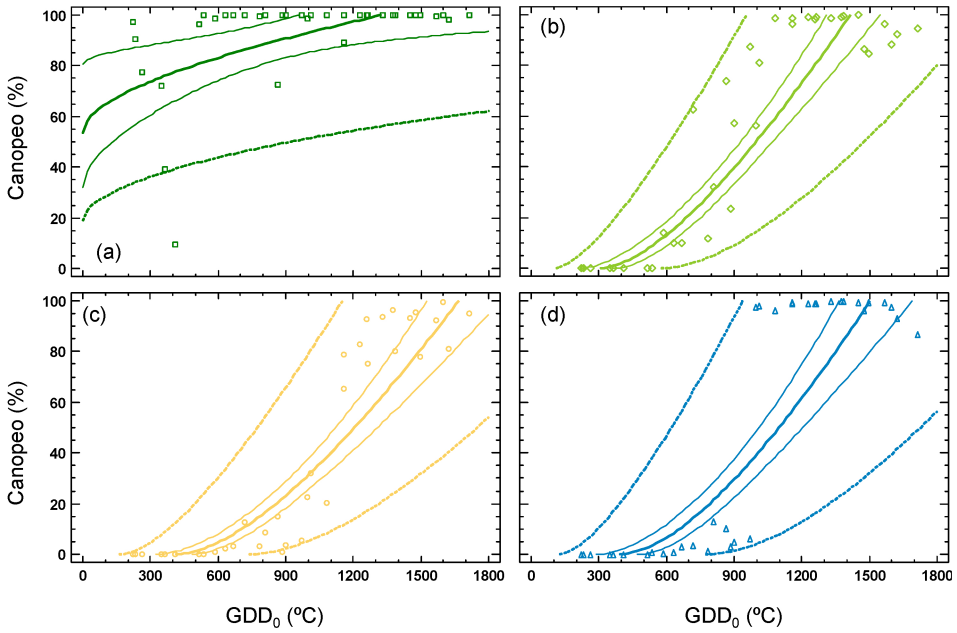


Figure 13. Individual regression models for different species/mixes with the Canopeo index: (**a**) dark green corresponds to the C3 mix, (**b**) light green corresponds to the C3/C4 mix, (**c**) yellow corresponds to C4 *Z. matrella*, and (**d**) blue corresponds to C4 *C. dactylon* × *C. transvaalensis*.

Table 5. A summary of the obtained mathematical models and their statistical significance for the different species for the Canopeo index.

Species [1]	a	b	Correlation Coef	R^2	*p*-Value
T	7.31281	0.07375	0.43	0.19	0.0083
R	−8.23203	0.484525	0.92	0.85	<0.0001
Z	−9.53005	0.478161	0.92	0.85	<0.0001
C	−10.1541	0.519619	0.90	0.80	<0.0001

[1] T corresponds to the C3 mix, R corresponds to the C3/C4 mix, Z corresponds to C4 *Z. matrella*, and C corresponds to C4 *C. dactylon* × *C. transvaalensis*.

The relationship between canopy cover and cumulative temperature (degree-days) was described using models of the form $Y = (a + b\sqrt{T_{cum}})^2$. In this formulation, the parameter a defines the baseline canopy cover at low thermal accumulation ($Y = a^2$ when $T_{cum} = 0$), while b determines the rate of change in response to the square root of cumulative temperature. The fitted models showed similar parameter values, with a ranging from −8.2 to −10.1 and b from 0.48 to 0.52 for R, Z, and C. Regarding the models

for T data, the obtained values (a equal to 7.0 and b equal to 0.07) differ from the models with data on C4 species. The models predict the presence of a marked minimum in canopy cover as cumulative temperature increases, reaching this minimum around 280–400 degree-days, corresponding to the zero-crossing of the term $\left(a + b\sqrt{T_{cum}GDD_0}\right)$. Beyond this threshold, the mathematical form of the model produces a slight recovery of canopy cover. Nevertheless, this increase should be interpreted cautiously, as it may reflect the limits of model structure rather than a true biological response. Overall, the results indicate that canopy cover decreases significantly with accumulated heat, highlighting the sensitivity of vegetation development to cumulative temperature during the growing period.

If we compare the obtained models graphically, as in Figure 14, we can clearly visualise the differences among species. According to the models, T reaches 100% coverage at 1328 °C, while the C4 species reach this value at 1416 °C for R, 1668 °C for Z, and 1504 °C for C. This moment corresponds to 01 May, 06 May, 20 May, and 12 May for T, R, Z, and C. Nevertheless, according to field data, it is possible to see that some plots reach the 100% or similar values (98 or 99%) of canopy at earlier moments with much lower temperatures: 538 for T (98.9%), 1080.5 °C for R (98.7%), 1600 °C for Z (99.4%), and 1012 °C for C (98.3%). This supports our observations of the models incorporating data: even though there is good accuracy, the change in canopy is much faster than the models are predicting. This is partially explained by the saturation of the canopy tool when values reach 100%. It is possible to establish a range of thermal accumulation for the period when the canopy evolves based on empirical data rather than the obtained models. These points are observed at about 1050 °C for R, 1200 °C for Z, and 1000 °C for C. These temperatures partially correspond to the temperatures at which the first values of the canopy equal to 100% were found for C and T, but not for Z. This is because the canopy increase in Z is slower than that in R and C.

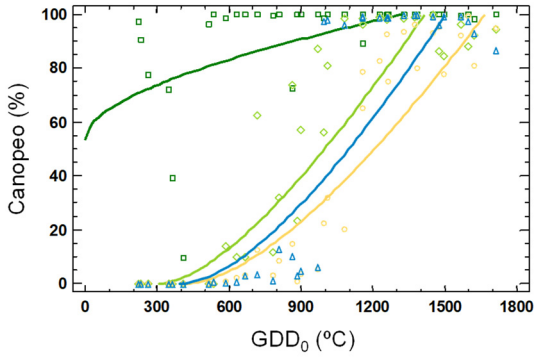


Figure 14. Comparison of regression models for different species/mixes with the Canopeo index: dark green corresponds to the C3 mix, light green corresponds to the C3/C4 mix, yellow corresponds to C4 *Z. matrella*, and blue corresponds to C4 *C. dactylon* × *C. transvaalensis*.

3.3.2. GLI

The obtained mathematical models that correlate the thermal accumulation with the GLI can be seen in Figure 15. These models follow a multiplicative equation in all cases, as shown in Equation (9). The obtained coefficients for the models, along with their correlation coefficients (R^2) and p-values, are shown in Table 6.

$$GLI = e^{(a+b\times\ln(Tcum))} \quad (9)$$

The relationship between the GLI and cumulative temperature (degree-days) is described using models of the form $GLI = e^{(a+b\times\ln(GDD_0))}$. In this formulation, the parameter a defines the baseline GLI at low GDD_0 ($Y = a^2$ when $T_{cum} = 0$), while b determines the rate of change in response to the cumulative temperature. The fitted models showed similar

parameter values for Z, R and C, with *a* ranging from −11.33 to −12.9 and *b* from 1.3 to 1.5. Nonetheless, the values for C3 turfgrass differ from the aforementioned values, with *a* equal to −3.7 and *b* equal to 0.3. The models predict a marked increase in GLI value as cumulative temperature increases. At low thermal accumulation values, the GLI is 0.12 for T and nearly 0 for other species. There are other important differences to be considered that are linked to the obtained models. The most important difference is the distinct thermal responses, which can be expressed as the increase in the GLI with temperature. The thermal response of T follows a decreasing pattern; the increase in the GLI accelerates quickly at low temperatures but slows at high temperatures. Meanwhile, Z, C, and R are characterised by an increasing rate of GLI growth with temperature. The increase in the GLI is higher when temperatures are elevated. These different increases in GLI rates among species are entirely consistent with the expected behaviour of C3 and C4 species, indicating that temperature sensitivities play a key role in spring green-up.

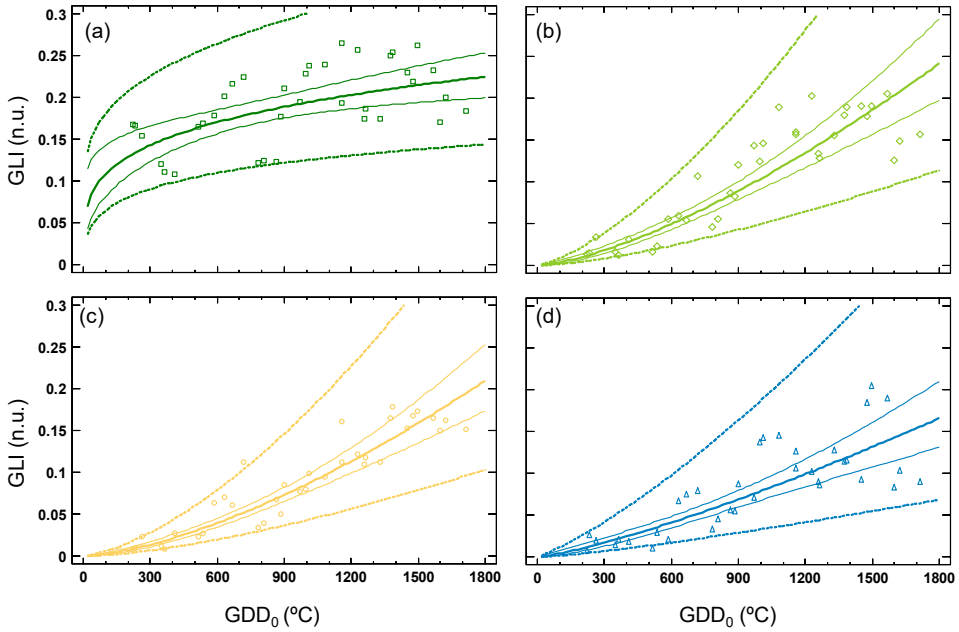


Figure 15. Individual regression models for different species/mixes with the GLI index: (**a**) dark green corresponds to the C3 mix, (**b**) light green corresponds to the C3/C4 mix, (**c**) yellow corresponds to C4 *Z. matrella*, and (**d**) blue corresponds to C4 *C. dactylon* × *C. transvaalensis*.

Table 6. A summary of the obtained mathematical models and their statistical significance for the different species for the GLI index.

Species [1]	a	b	Correlation Coefficient	R^2	*p*-Value
T	−3.38677	0.252634	0.57	0.32	0.0004
R	−12.2104	1.43933	0.92	0.85	<0.0001
Z	−12.9547	1.51977	0.94	0.88	<0.0001
C	−11.3313	1.27182	0.87	0.76	<0.0001

[1] T corresponds to the C3 mix, R corresponds to the C3/C4 mix, Z corresponds to C4 *Z. matrella*, and C corresponds to C4 *C. dactylon* × *C. transvaalensis*.

Comparing the obtained models, shown in Figure 16, we can clearly visualise the differences among species. If we compare the GLI model of T with those for other species, it is possible to predict the moment at which other models will achieve a higher GLI than T. This moment corresponds to a GDD_0 of 1695 °C for R, 1902 °C for Z, and 2428 °C for C. According to the climatological meteorological data for the year, this thermal accumulation was reached on 21 May for R, 30 May for Z, and beyond the considered period for C.

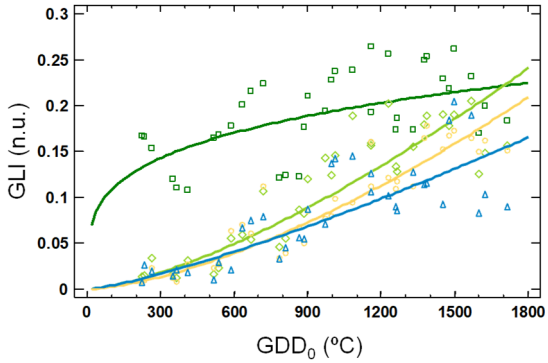


Figure 16. Comparison of regression models for different species/mixes with the GLI index: dark green corresponds to the C3 mix, light green corresponds to the C3/C4 mix, yellow corresponds to C4 *Z. matrella*, and blue corresponds to C4 *C. dactylon* × *C. transvaalensis*.

3.3.3. Greenness Index

In the following paragraphs, the mathematical models obtained are described, which correlate the thermal accumulation with the proposed greenness index. These correlations can be seen in Figure 17. These models follow a Logarithmic equation in all cases, as shown in Equation (10). The obtained coefficients for the models, along with their correlation coefficients (R^2) and *p*-values, are shown in Table 7.

$$Greenness = a + b \times \ln(Tcum) \quad (10)$$

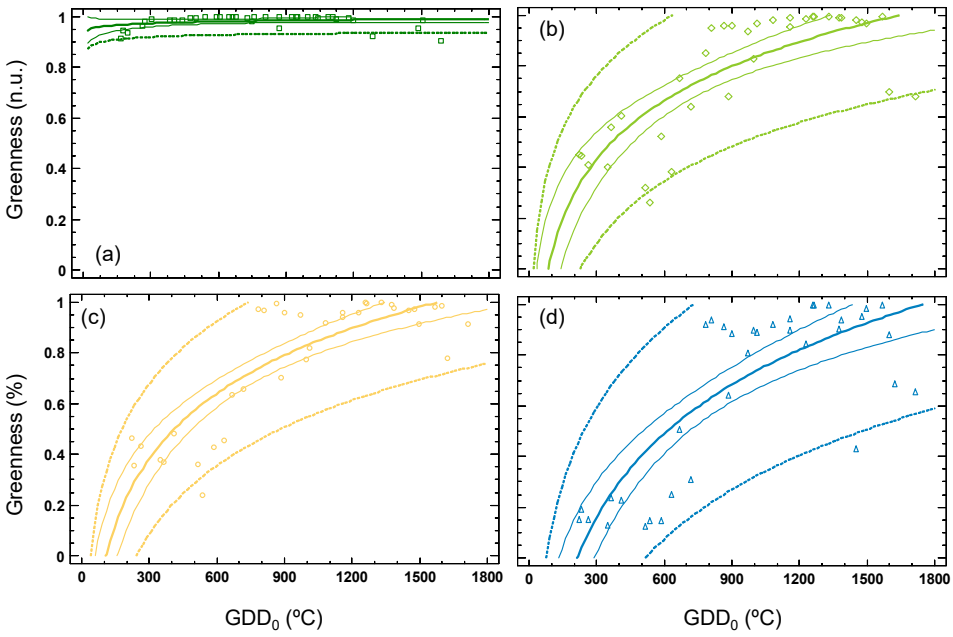


Figure 17. Individual regression models for different species/mixes with the greenness index: (**a**) dark green corresponds to the C3 mix, (**b**) light green corresponds to the C3/C4 mix, (**c**) yellow corresponds to C4 *Z. matrella*, and (**d**) blue corresponds to C4 *C. dactylon* × *C. transvaalensis*.

The relationship between the greenness of the turfgrass and cumulative temperature (degree-days) is described using models of the form $Greenness = a + b \times \ln(GDD_0)$. In this formulation, the parameter a defines the baseline greenness at low GDD_0 ($Y = a$ when $T_{cum} = 0$), while b determines the rate of change in response to the cumulative temperature. The fitted models show similar parameter values for Z, R and C, with a ranging from -1.5 to -2.5 and b from 0.33 to 0.47. Nonetheless, the values for C3 turfgrass differ from the aforementioned values, with a equal to 0.9 and b equal to -0.01. The models predict a

progressive increase in the greenness index as the cumulative temperature rises. At low temperature values, the greenness for species T is relatively high compared to the others, and its variation is barely insignificant with increasing temperature. Meanwhile, R, Z, and C start with much lower greenness values. Nonetheless, important differences arise due to differences in temperature sensitivity among species. Species T shows a nearly flat response, with the index value increasing very slowly as temperature grows, indicating low necessity of thermal accumulation, which is aligned with the expected behaviour of C3 species in the given climatic zone with no green colour loss during winter. In contrast, species R, Z, and C show a strongly positive slope, indicating that their greenness increases at higher temperatures, as expected for C4 species during spring green-up. Among the C4 plots, C shows the more pronounced increase, followed by Z and R, reflecting the strongest dependence on temperature. Nevertheless, C is the species that starts the increase at higher accumulated temperatures.

Table 7. A summary of the obtained mathematical models and their statistical significance for the different species for the greenness index.

Species [1]	a	b	Correlation Coefficient	R^2	*p*-Value
T	0.913959	0.010076	0.23	0.05	0.1587
R	−1.47003	0.333631	0.79	0.62	<0.0001
Z	−1.73506	0.371384	0.85	0.72	<0.0001
C	−2.55281	0.475845	0.81	0.66	<0.0001

[1] T corresponds to the C3 mix, R corresponds to the C3/C4 mix, Z corresponds to C4 *Z. matrella*, and C corresponds to C4 *C. dactylon* × *C. transvaalensis*.

The obtained models are compared graphically in Figure 18. We can clearly visualise the differences among species. If we compare the greenness model of T with those for other species, it is possible to predict the moment at which other models will achieve higher greenness than T. This moment corresponds to a GDD_0 of 1585 °C for R, 1528 °C for Z, and 1708 °C for C. According to the climatic meteorological data of the year, this thermal accumulation was reached on 17 May for R, 13 May for Z, and 22 May for C.

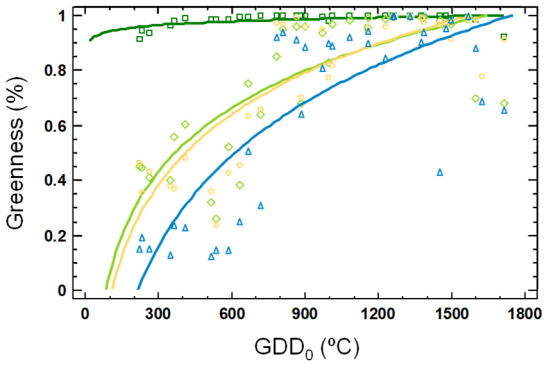


Figure 18. Comparison of regression models for different species/mixes with the greenness index: dark green corresponds to the C3 mix, light green corresponds to the C3/C4 mix, yellow corresponds to C4 *Z. matrella*, and blue corresponds to C4 *C. dactylon* × *C. transvaalensis*.

3.3.4. Homogeneity Index

In the following paragraphs, the obtained mathematical models that correlate thermal accumulation with the proposed homogeneity index are described. These correlations are shown in Figure 19. These models follow a Logarithmic equation in all cases, as shown

in Equation (11). The obtained coefficients for the models, along with their correlation coefficients (R^2) and *p*-values, are shown in Table 8.

$$Homogeneity = a + b \times \ln(Tcum) \quad (11)$$

The relationship between the homogeneity of the turfgrass and cumulative temperature (degree-days) is described using models of the form $Homogeneity = a + b \times \ln(GDD_0)$. In this formulation, the parameter a defines the baseline homogeneity at a low GDD_0 ($Y = a$ when $T_{cum} = 0$), while b determines the rate of change in response to the cumulative temperature. The fitted models show similar parameter values for Z, R and C, with a ranging from −3.1 to −4.7 and b from 0.69 to 0.83. Nonetheless, the values for C3 turfgrass differ from the aforementioned values, with a equal to 0.9 and b equal to 0.19. These values indicate that C3 species are characterised by a high baseline homogeneity, almost 1. Meanwhile, the C4 species at low temperatures have extraordinarily low values, below −1, which is the mathematical minimum of the equations. Thus, it indicates that the model needs to be better fitted for low thermal accumulation for C4 species.

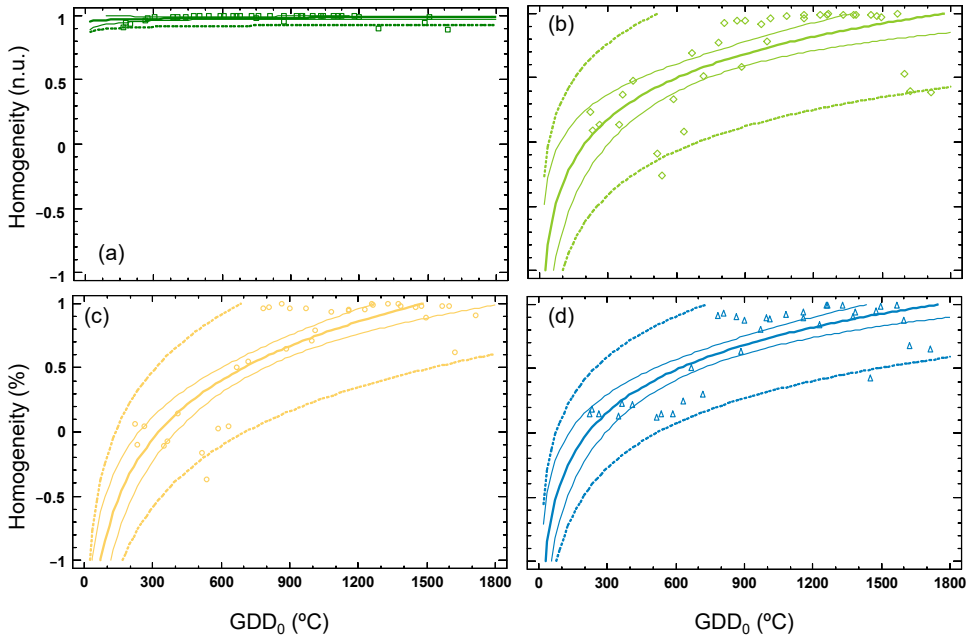


Figure 19. Individual regression models for different species/mixes with the homogeneity index: (**a**) dark green corresponds to the C3 mix, (**b**) light green corresponds to the C3/C4 mix, (**c**) yellow corresponds to C4 *Z. matrella*, and (**d**) blue corresponds to C4 *C. dactylon* × *C. transvaalensis*.

Table 8. A summary of the obtained mathematical models and their statistical significance for the different species for the homogeneity index.

Species [1]	a	b	Correlation Coefficient	R^2	*p*-Value
T	0.927179	0.00811998	0.17	0.03	0.3184
R	−2.45182	0.461395	0.70	0.49	<0.0001
Z	−3.8066	0.658087	0.84	0.71	<0.0001
C	−5.70233	0.911321	0.83	0.69	<0.0001

[1] T corresponds to the C3 mix, R corresponds to the C3/C4 mix, Z corresponds to C4 *Z. matrella*, and C corresponds to C4 *C. dactylon* × *C. transvaalensis*.

The obtained models indicate a progressive increase in the homogeneity index with increasing cumulative temperature. At low temperature values, the homogeneity for species T is relatively high compared to the others, and its variation is barely insignificant

with the increase in temperature, as expected for C3 species with no dormancy. Meanwhile, R, Z, and C start with much lower homogeneity values due to the dormancy period and leaf greenness loss. Nevertheless, there are important differences in temperature sensitivities among species. The mixture T shows an almost flat response. The homogeneity index values increase very slowly as the temperature rises, indicating a low necessity for thermal accumulation, as expected. In contrast, the C4 species are characterised by a strongly positive slope, indicating that their homogeneity accelerates at higher temperatures, as expected in C4 species during spring green-up, when green colour appears slowly until it covers the entire grass surface. In this case, the species with the highest increase rate is Z, followed by C and R.

If we compare the obtained models graphically, as shown in Figure 20, we can clearly visualise the differences among the species. If we compare the homogeneity model of T with those for other species, it is possible to predict the moment at which other models will achieve higher homogeneity than T. This moment corresponds to a GDD_0 of 1728 °C for R, 1455 °C for Z, and 1541 °C for C. According to the climatic meteorological data of the year, this thermal accumulation was reached on 23 May for R, 9 May for Z, and 14 May for C.

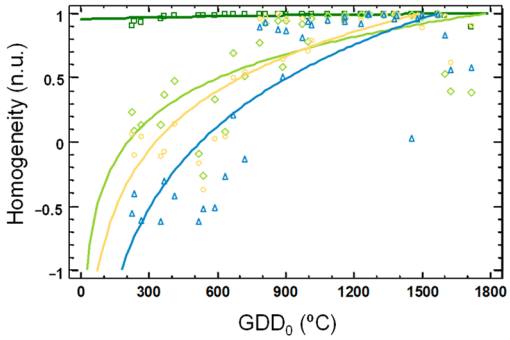


Figure 20. Comparison of regression models for different species/mixes with the homogeneity index: dark green corresponds to the C3 mix, light green corresponds to the C3/C4 mix, yellow corresponds to C4 *Z. matrella*, and blue corresponds to C4 *C. dactylon* × *C. transvaalensis*.

4. Discussion

4.1. Differences in Spring Green-Up of Studied Species and Differences Among Microclimatic Sectors

4.1.1. C3/C4 Mix (R Plots)

The periodic visits to the field trials indicate that R plots started spring green-up in the sector with warmer temperatures early, on 1 February 2024, while in the coldest sector this start was delayed until 28 February 2025, almost one month later. Complete coverage with the C3 seeds of the R plots became difficult to assess. The distribution of seeds and the resulting spatial pattern of canopy greening were non-homogeneous, resulting in an irregular pattern of green colouration.

On about 11 April 2025, the R plots of the warmest sector were characterised by fully grown C3 grasses, even though these did not cover the entire plot. Meanwhile, in the coldest plots, the C3 species of the R mixture were fully grown from 22 April 2025 to 28 April 2025. In the case of the coldest plots, canopy development and early green-up were even more irregular, with some plots having only a few grown individuals. In colder plots, sector 3 registered low temperatures similar to those in sectors 2 and 1. Nevertheless, the number of hours that turfgrass remained at low temperatures was higher in more exposed plots, namely sectors 2 and 3. In February, plots in sector 1 experienced negative temperatures for 123 h, while plots in sector 2 and sector 3 experienced temperatures for 153 and 164 h. Thus, besides having the lowest maximum temperatures, these plots also

have the lowest minimum temperatures. These microclimatic differences might be crucial in the irregular germination of C3 seeds.

The microclimatic effects of temperature on seed germination have been widely studied in plants of cold climates [46,47]. Additionally, several studies demonstrate a delay in the germination of cool-season turfgrasses at low temperatures [48]. The delayed germination can be as long as 14 to 16 days in the case of *F. arundinacea* and *L. perenne* [49] and *P. pratense* [50]. It must be noted that these studies were conducted under controlled conditions, with either stable or varying temperatures, and germination was measured rather than spring green-up or canopy development. Nevertheless, the delay in germination reported in the literature and slower growth under cold conditions can partially explain the delay in green canopy presence registered in this study. In the case of the present study, conducted under real conditions with microclimatic differences, visible green-up in the coldest plots was delayed by up to 28 days in the most favourable plot. This delayed onset of visible green-up under low-temperature conditions can partially explain the irregular spatial patterns of canopy development of C3 observed in the plots of sector 3.

4.1.2. C3 Mix (T Plots)

The observed phenology in the T mixture, composed solely of C3 grasses, with no colour loss during dormancy, presented no clear visual differences among microclimatic sectors. There was a slight colour change due to the growth of new leaves, which occurred simultaneously across all sectors. Therefore, it is possible to say that, in contrast to germination responses reported under controlled conditions, the studied microclimatic variation in temperature did not affect the start of spring green-up, i.e., the visible appearance of new leaves of an existing plant, of C3 species in the T mixture. The appearance of new leaves occurred in late February, coinciding with the date at which C3 species became visible in the R mixture in the worst microclimatic region. Thus, the earlier green-up of C3 species in the R mixture (pre-existing C4 grasses) compared to the T mixture (pre-existing pure C3 turfgrass) can be explained by the differences in canopy structural dynamics during winter dormancy, rather than by differences in physiological activation. In C4 mixtures, such as R, senescent leaves lose pigmentation and water content, resulting in reduced leaf volume and canopy height, and increased canopy openness, which allows newly emerging C3 leaves to become visible earlier.

In contrast, in pure C3 mixtures, such as T mixture, leaves retain their colour and hydration, maintaining canopy density throughout the winter. As a result, emerging C3 leaves must elongate further before they become detectable, thereby delaying the apparent onset of green-up. These differences highlight the roles of previous canopy structure and conditions and leaf senescence in modulating the phenological visibility of spring green-up, both visually and through vegetation indices, rather than underlying differences in growth initiation. Previous studies demonstrated a reduction in leaf area when dormancy was triggered in C4 species [51], which directly impacts canopy structure.

4.1.3. C4 Monocultures (Z and C Plots)

Among C4 turfgrass species, Z and C, even though Z presented green leaves during field visits earlier than 14 March 2025, these leaves were confined to the basal area of the plant and were not visible at the canopy level. Therefore, these leaves were not captured by vegetation indices, which rely on canopy-level reflectance and do not reflect the actual onset of spring green-up. Previous studies conducted in Mediterranean and European transition-zone environments have documented partial winter colour retention and shorter dormancy periods in *Zoysia matrella*, particularly in fine-leaf cultivars such as 'Zeon', under mild winter conditions and favourable microclimatic conditions [52,53], which aligns with

the evidence observed during field visits. Nevertheless, indexes do not reflect this initial moment of the spring green-up. Significant growth did not characterise these new leaves, which remained in the basal area of the plant, covered by leaves without green colouration. Thus, their presence was not evident in the canopy, and therefore, the indices did not report this evidence. The spring green-up process was slower and took longer to reach a high level of green colouration. The moment at which Z plots reached a high level of green colouration fell between 22 April 2025 and 28 April 2025. This resulted in a prolonged duration of the initial phases of spring green-up, with a duration of more than one month. This extremely long duration in the initial phases of spring green-up can be attributed to the succession of rainy days during March and April, with low radiation and reduced high daily temperatures, indicating the importance of high daily temperatures for spring green-up rather than low temperatures.

In that moment, Z has a green colouration; moreover, its uniformity of spring green-up varies along the sector. While in sector 1, almost the entire plot was completely green, in sector 2, and particularly Sector 3, there were some parches with no spring green-up, indicating an irregular exit from dormancy. These differences are not easily explained by the temperatures in April, since the differences among microclimatic conditions are almost null in this month. The minimum and maximum temperatures in each sector are almost the same, with a higher average temperature in sector 3 (13.1 °C) than in sectors 2 and 1 (12.3 °C and 12.8 °C, respectively). Thus, this effect can be explained by the most severe conditions recorded in January and February, which might affect the survival of certain individuals during the dormancy period. The lowest temperatures registered in the plots during January and February are similar. The time that plots remain below 5, 0, and −5 °C is slightly different among plots and is higher in Sectors 2 and 3. This can be a possible explanation for the observed irregular germination caused by winterkill due to abiotic stress. Several authors have reported the effect of low winter temperatures on winterkill of C4 species, particularly in *Z. matrella* [54], and in the Zorro cultivar, indicating a freeze tolerance of −9 °C [55,56]. The minimum temperature reached was equal across all plots (−11 °C). This implies that typical equations that use minimum temperature to calculate or estimate survival rates should be applied carefully, and it might be more interesting to use continuous data rather than minimum and maximum punctual temperatures.

Regarding the C plots, these showed initial green leaves later than in Z, but once the green leaves appeared, the spring greening process accelerated faster than in Z, reaching a homogeneous green colouration on 11 April 2025, with remarkable colour variation only in 1 week. The first evidence of green leaves was visible on 4 April 2025. As opposed to what occurred in Z, the C leaves grew with greater density, provoking faster spring green-up than Z. It must be noted that 31 March was the last date on which temperatures fell below 0° C. A couple of days later, the first leaves of C appeared, indicating a possible impact of minimum temperatures, in addition to thermal accumulation, on triggering spring green-up. Additionally, it is important to note that, unlike what has been observed in Z, the C plots did not show irregular leaf emergence, indicating a lower impact of winterkill. Traditionally, C was more susceptible to winterkill than Z [57]. Nevertheless, in the case of tested cultivars, the effect of winterkill on spring green-up uniformity was greater for the *Z. matrella* cultivar Zorro than for *C. dactylon* × *C. transvaalensis* cultivar Texoma (OKC1876).

4.1.4. C3/C4 Mix Compared with C4 Monoculture

Considering the obtained results, comparing R with C in the C3/C4 mixes, if C3 overseeding is conducted in winter or spring, the impact on spring green-up will be almost null. Even though the start of spring green-up in the plot was earlier for R than for C, the end of spring green-up occurred approximately on the same date according to field visits.

Regarding the indices and the obtained models, the Canopeo model indicated that the moment at which C plots accelerated was at a DGG_0 equal to 1000 °C, whereas for R plots it was at 1050 °C.

Comparing the values of the greenness and homogeneity indices, as well as the obtained models, the behaviour of the R plots is highly similar to that of the Z plots, with an early start of spring green-up but prolonged spring green-up in the initial stages. Thus, overseeding must be conducted at the end of summer or early in autumn, ensuring germination and leaf emergence before winter. Otherwise, the impact of overseeding in spring green-up is minimal.

4.2. Differences Among Obtained Models

4.2.1. The Best Model to Determine the Ending of the Initial Stages of Spring Green-Up

There is one key index that has proven its ability to determine the end of the initial stages of spring green-up, the moment when all or almost all of the plot is covered with green vegetation. This is the Canopeo index, which determines the fraction of the surface covered in green, regardless of the intensity of the green canopy. In Table 9, we have included the dates of the start and end of the initial stages of spring green-up across the different plots, along with the thermal accumulation. Moreover, the accumulated temperature at which Canopeo models accelerate is also included. It is possible to see a clear comparison between the field-determined end of the initial spring green-up process and the GDD_0 temperature at which Canopeo models accelerate.

Table 9. A summary of the start and end of the initial stage of spring green-up and their relation with Canopeo models.

Species [1]	Start of Spring Green-Up		End of Spring Green-Up		GDD_0 at Which Canopeo Models Accelerate (°C)
	Date	GDD_0 (°C)	Date	GDD_0 (°C)	
T	28 February 2024	547	28 February 2024	547	
R	1 February 2024	249	11 April 2025	1013	1050
Z	4 April 2025	916	22 April 2025	1180	1200
C	4 April 2025	916	11 April 2025	1013	1000

[1] T corresponds to the C3 mix, R corresponds to the C3/C4 mix, Z corresponds to C4 *Z. matrella*, and C corresponds to C4 *C. dactylon* × *C. transvaalensis*.

The rest of the models do not perform efficiently in predicting the end of this starting point, since at this moment, the greenness of the plots is low, and the remaining indexes do not measure green coverage but the intensity of this green coverage. Thus, the other indices are not suitable for determining this initial moment of spring green-up. Although model predictions tend to show a slight delay relative to the observed green-up dates, they successfully capture the relative temporal dynamics, the impact of small-scale temperature variability, and differences among species, which are the main focus of this study.

4.2.2. The Best Model to Determine the Moment at Which C4 Species Overtake C3 Species

Among the models used to evaluate when the greenness of the C4 species surpasses that of the C3 species, the best results are mainly linked to the indices evaluating the greenness of the turfgrass. These indices are the GLI and the two previously proposed indices [39], greenness and homogeneity. In Table 10, we have included the accumulated temperature at which each C4 species or the C3/C4 mix reached the C3 mix value.

For R mix, the three models yield similar temperatures (a variation of only 6 days) between 17 and 23 May. The gathered images and field visits from 22 May to 05 June demonstrate a similar colouration in R and T plots. The main observed differences between these plots are the irregular growth of C3 grasses in the R plots, caused by the irregular

germination. So, from this point, differences are merely in terms of plant growth rather than plant colour. Given the extremely small differences among predictions in models, it is difficult to select the best model for R, and apparently, all models are correct.

Table 10. GDD_0 and the day on which each species overtakes the values of T.

Species [1]	GLI		Greenness		Homogeinity	
	GDD_0 (°C)	Date	GDD_0 (°C)	Date	GDD_0 (°C)	Date
R	1695	21 May	1585	17 May	1728	23 May
Z	1902	30 May	1528	13 May	1455	9 May
C	2428	-	1707	22 May	1541	14 May

[1] R corresponds to the C3/C4 mix, Z corresponds to C4 *Z. matrella*, and C corresponds to C4 *C. dactylon* × *C. transvaalensis*.

Regarding the plots with the *Z. matrella* cultivar Zorro (Z), there is considerable divergence among models. While the homogeneity model indicates that these plots reached the same characteristics as T plots on 9 May, the GLI delays this date to 30 May, and the greenness models offer an intermediate date of 13 May. According to field visits, the visual aspect of colour is similar in Z and in T on 19 May. On 12 May, even though the leaf colouration of Z is similar to that of T, the Z plots show incomplete coverage by green leaves. Thus, the homogeneity models fail as they determine the date too early. Meanwhile, the GLI identifies this point in June, later than field registers indicate.

Finally, in the case of C, which is the most complex one, two of the models indicate the moment with a one-week difference (greenness and homogeneity) at the middle to end of May, while the GLI places that moment beyond the collected temperature data (probably the middle of June). This difference is caused by the particular colouration of *C. dactylon* × *C. transvaalensis*, which tends toward bluish colours, and the way in which different indices operate. While the proposed indices used only the green band of the image to determine the intensity of green, the GLI combines this information with the blue and red bands. The field visits conducted from 22 May to 05 June indicate that the visual appearance of C does not differ from that of T in terms of coverage and density, even though the colouration differs. Thus, as in the case of Z, GLI models indicate the latter date that the field data demonstrate.

According to the analysed data, it is possible to say that the best models to determine the moment at which each plot has reached its optimal colouration, when it surpasses or nearly surpasses that of T, are those based on greenness. The differences among models are minimal for R but crucial for Z and C. Models based on homogeneity data tend to place the moment earlier than observed, whereas those based on GLI data indicate that the moment is later.

4.2.3. Best Index to Assess Differences Between Species and Between Sectors

According to the data provided in Section 3.2, we can compare which index is best for identifying differences among turfgrasses. The Canopeo index was able to identify differences between species in 11 out of 13 moments and failed in identifying differences among sectors, being able to do so just in the last image. With the GLI, it was feasible to identify differences among species across all included periods and among sectors in almost half of the periods (6 out of 13). Regarding the proposed indices, the greenness index identified differences between species in 8 out of 13 images and differences between sectors in only 2 cases, whereas homogeneity data differentiated species in 6 out of 13 images and sectors in only 3 cases. Thus, the best index for phenotypic species or for determining the impact of microclimatic differences is the GLI, which has proved to be the most effective.

4.3. Observed Microclimatic Effect in Colour Decay at End of Trial

Beyond the already mentioned microclimatic temperature effects during spring green-up, an additional effect has been observed: an inversion of tendencies at the end of the trials. The plots that go into spring green-up earlier (Sector 1) have shown a reduction in colour and even coverage, as indicated by the Canopeo index.

The earlier green-up observed in plots of sector 1 compared to plots of sectors 2 and 3 has been attributed to microclimatic differences in temperature among plots, as explained above. Sector 1 consistently recorded higher average temperatures and spent less time under critical temperature thresholds (below 0 °C or 5 °C) during January and February, creating a more favourable thermal environment for an early metabolic activation of turfgrass species. These microclimatic variations, likely driven by surrounding structures, explain why phenological timing diverged among sectors despite the uniform management.

Nonetheless, this early activation of plots in sector 1 did not result in an enhanced visual quality at the end of the trial. The prolonged rainfall and low radiation during March and April imposed severe physiological constraints on plots that had started green-up early. These constraints include carbohydrate reserve depletion under suboptimal photosynthetic conditions and potential hypoxia conditions in root zones due to saturated soils after prolonged rain. On the contrary, later-greening plots synchronised their growth with improved environmental conditions, allowing for more efficient nutrient uptake and sustained colour. This observed contrast indicates that while microclimatic variations in temperature strongly influence the timing of green-up, their benefits can be easily offset by adverse weather patterns during early spring, jeopardising the quality of turfgrass in summer. Therefore, microclimatic conditions should be studied and incorporated into the design and management of turfgrass surfaces in urban green areas. Other authors have reported similar effects, linked to early spring phenology, on reducing vegetation growth rates during the green-up period in temperate forests due to climate change [58].

4.4. Impact for Urban Science and Green Infrastructure Management in Climate Change Scenarios

In recent years, several urban studies have focused on thermal variation or thermal gradients in cities, including both the UHI and intra-urban small-scale gradients. Moreover, for efficient climate adaptation in urban green areas, understanding how small-scale thermal variability within urban green spaces affects vegetation performance is essential for developing resilient strategies for green infrastructure design and management under ongoing urban warming. As stated in the Section 1, in the framework of this paper, the studied temperature gradient refers to small-scale temperature differences within a single peri-urban green space, rather than to continuous spatial gradients or urban–rural contrasts.

Previous studies have demonstrated a microclimatic temperature gradient of 1.29 to 2.71 °C in urban green areas in Beijing [59], while the gradient in Perugia was −1.1 to 1.3 °C [36]. A recent study of the UHI effect in Madrid found increases of 1 °C during the day and 2 °C during the night [60]. Thus, our gradient aligns with the reported values, and the observed differences in delaying spring green-up, amounting to about 1.5 °C, can be easily translated to urban areas with these reported gradients for the UHI, including Madrid. Moreover, other authors have reported decreases in temperature in green areas in urban regions [61,62] and park cooling gradients [63]. Moreover, climate change will affect average temperatures, leading to variations in green-up and other phenological events, as noted by various authors [64,65]. According to a recent publication, an increase of 1.4 °C in average temperatures in Spain is expected by 2050 [66]. Therefore, the studied temperature gradient and the obtained models can be applied in future CC scenarios as well as to intra-urban variability patterns caused by different structures, materials, and vegetation canopies. While the present study does not aim to quantify the UHI effect itself, it contributes to

the literature by showing that temperature differences of a similar magnitude occur at intra-urban and sub-park scales, and these can induce substantial phenological shifts typically associated with larger-scale urban warming. This paper provides experimental evidence linking small-scale thermal variability to vegetation phenology, a relationship often assumed but rarely quantified at this spatial scale.

Thus, we can expect an increase in future temperatures, and having information about green areas' vegetation response to that increase is key to adequate management and planning. The provided models provide a valuable tool for predicting spring green-up onset to plan for green infrastructure management and resource allocation. Advancing spring green-up might imply longer irrigation and mowing periods and higher frequency for cool-season species, which directly affect maintenance costs. In these species, the temperature gradient advances or delays spring green-up by one month. On the contrary, early spring green-up for warm-season grasses also implies a longer period of use of turfgrass by citizens and a lower period with dormancy colour. This can affect citizens' acceptance of warm-season species in Madrid's continental climate, allowing for the use of species better adapted to water scarcity. It should be noted that temperature gradients have little effect on spring green-up in these species. Thus, adequate species selection, accounting for spring green-up modifications, is necessary to ensure the sustainability of green areas. The inclusion of green areas is vital to reduce the compactness of urban cores and provide a more sponge-like urban morphology, facilitating the formation of microclimates [67] and improving citizens' comfort in urban areas. Nonetheless, these areas must be climate-resilient spaces with reduced management costs in future CC scenarios. In this context, the present study contributes to urban climate research by providing field-based evidence of how microclimatic thermal differences, comparable in magnitude to projected warming, translate into measurable phenological shifts in managed vegetation at scales relevant for urban design and management. Selecting the best species, which entails understanding their phenological behaviour during spring green-up under different temperatures, is one of the key adaptation measures to be considered in urban green areas.

For urban climatologists, the reported results highlight that small-scale thermal heterogeneity within urban and peri-urban areas, provoked by local structures, materials, and surface characteristics, is often overlooked in city-scale analyses and can generate functional vegetation responses comparable to those attributed to the urban heat island effect. Therefore, these patterns should be studied locally and considered by experts during the design phases of urban green areas and green infrastructure management. Moreover, these findings are particularly relevant for urban climate studies, where vegetation responses are typically modelled at coarser spatial resolutions, potentially overlooking the effects of small-scale thermal variability.

4.5. The Potential Implications of Soil Moisture in Spring Green-Up at a Microclimatic Scale in Green Areas

Given that multiple studies in the literature indicate that, in grasslands, the impact of SM can exceed that of temperature, it is necessary to discuss this issue, focusing on gardens and urban environments. Multiple studies indicate that, although temperature is the primary trigger for spring green-up in cold regions [68], in warmer regions SM becomes more important [69–71]. The results obtained in these studies are global or regional, based on remote sensing data, and include no studies of microclimatic conditions, urban regions, or green areas; they focus on natural regions whose SM is rain-dependent. Moreover, these studies do not offer SM results that can be compared with SM measured with handheld devices. In the present study, data were obtained with handheld devices, and the studied surface has smaller dimensions, allowing for deeper investigation of the microclimatic conditions.

Data collected on different dates, 2 April and 22 May, indicated that soil moisture was lower in plots that experienced green-up early, with average values of 13.8% in sector 1 compared with 14.3 and 16.6% in sector 2 and sector 3 on 2 April. This moment corresponds with the start of spring green-up for the C4 species. In the latter period, on 22 May, this trend is maintained, with lower SM values in sector 1 (21.5%) than in sector 2 (22.9%) and sector 3 (25.2%). These results contradict the aforementioned references, which stated that the trigger for spring green-up was an increase in soil moisture. In our results, the plots that started spring green-up first are those with the lowest SM. This might be explained by the local increase in canopy and surface temperatures, which increases the rate of soil water evaporation, decreasing the SM. Furthermore, SM variability at a local scale is more closely related to design factors, such as generated orography, projected shadows, and surrounding materials and structures. All these factors also affect canopy temperature, generally leading to higher temperatures in areas with lower SM due to differences in soil water evaporation, as stated before. Thus, existing models that highlight the primary role of SM in spring green-up in grasslands do not apply to urban green areas with microclimatic variability resulting from design or surrounding conditions.

Additionally, the study year was a period of high rainfall, and soil moisture was not a limiting factor. This can be aligned with the situation in green areas, where irrigation ensures that SM is never the limiting factor for vegetation development. Thus, in regions where soil moisture is consistently maintained within an optimal range, such as in wet years or under irrigation, its role as a limiting factor is reduced, and therefore its influence on the triggering of spring green-up is expected to be less pronounced.

4.6. Limitations of Conducted Tests

The main limitations of the conducted test are described and justified in the following paragraphs. The first limitation is that the data are from a single season. Data may be limited due to a rainy period during the trial or to particularly low or high temperatures in this year, which can affect model accuracy in other periods. Nevertheless, given the microclimatic variation in temperature across plots and the large number of plots, the data can be considered representative of the trends expected in the future. While the use of RGB imagery under varying illumination conditions may affect vegetation indices, steps were taken to ensure consistency in image acquisition. Additionally, some of the indices used (GLI and Canopeo) are relatively robust to moderate changes in lighting. Therefore, the results should be interpreted with caution, particularly when considering absolute values.

In addition to the aforementioned limitations, temperature levels were not independently replicated; each microclimatic block represents a single realisation of each condition. Therefore, the presented results should be interpreted as strong evidence of temperature-associated patterns rather than definitive causal effects. Nevertheless, the results of the spring green-up comparison among different turfgrass species within each block are robust to this limitation, allowing for a reliable assessment of interspecific differences in phenological responses.

Other limitations include the inclusion of a single cultivar of each of the studied species, which might limit the applicability of these conclusions and the obtained models to other cultivars of the same species. We have conducted our study with two of the newest, which are currently commercialised in Spain. In future work, we will include data on additional cultivars of C4 turfgrasses.

5. Conclusions

Microclimatic gradients in urban areas are important, and multiple surrounding surfaces affect temperature ranges. In turfgrass, these microclimatic gradients affect spring-

up and need to be considered in the design and management of urban green areas. In this paper, we have evaluated the effect of a microclimatic temperature gradient induced by a wall perpendicular to the main wind direction in winter.

Our results indicate that, for cool-season turfgrasses, the studied temperature gradient delayed the onset of spring green-up by 1 month. On the contrary, differences in the timing of spring green-up in warm-season turfgrasses were lower. Nonetheless, in both cool-season and warm-season, the microclimatic temperature range affected the homogeneity of spring green-up, which was lower in the coldest sector. The lowest temperatures might affect the canopy of cool-season seeds and might cause winterkill in *Z. matrella* cultivar Zorro. No effects have been found on the homogeneity of spring green-up on previously established cool-season turfgrasses and on *C. dactylon* × *C. transvaalensis* Texoma (OKC1876). Mathematical models of spring green-up, when compared with accumulated temperature, showed a good fit, as indicated by R^2 values. The best model to predict the complete green coverage of the plots is the one based on the Canopeo index. Meanwhile, the best models for estimating the moment at which warm-season turfgrasses reach the colouration of cool-season turfgrasses were those based on the proposed greenness index. Data obtained via the GLI accurately demonstrate their capacity to phenotype the species and to differentiate among temperature gradient sectors, as shown by multifactorial ANOVAs.

In future work, the impact of summer water stress on the spring green-up process and the possible benefits of natural-based products in accelerating it for warm-season turfgrasses will be studied. Moreover, additional data will be collected to validate these models in other locations characterised by different climates and to assess the impact of photoperiod on the start and end points of spring green-up.

Author Contributions: Conceptualisation, J.M. and L.P.; methodology, L.P.; software, L.P.; validation, J.M.; formal analysis, L.P.; investigation, J.M., A.C. and L.P.; resources, P.V.M.; data curation, L.P.; writing—original draft preparation, M.d.P.G.d.P. and L.P.; writing—review and editing, L.P. and A.C.; visualisation, J.M.; supervision, L.P. and A.C.; project administration, P.V.M. funding acquisition, P.V.M. All authors have read and agreed to the published version of the manuscript.

Funding: This research was funded by Comunidad de Madrid, grant number FP24-GREENNATUR.

Institutional Review Board Statement: Not applicable.

Informed Consent Statement: Not applicable.

Data Availability Statement: Data can be requested via email to authors.

Acknowledgments: During the preparation of this manuscript, the authors used Grammarly (version number: 1.157.0.0) for the purposes of English revision. The authors have reviewed and edited the output and take full responsibility for the content of this publication.

Conflicts of Interest: Jose Marin is affiliated with a private company (ÁreaVerde MG Projects S.L.) operating in the turfgrass sector. This affiliation did not influence the results or conclusions of the study. The authors declare no conflict of interest.

Appendix A

Table A1. Average values and assigned groups for multifactorial ANOVA for different dates using green canopy coverage tool. Different lowercase letters indicate significant differences (LSD test, $p < 0.05$).

Date	C	Z	R	T	*p*-Value	S1	S2	S3	*p*-Value
31 January 2025	0.0119333 [a]	0.0058111 [a]	0 [a]	88.3545 [b]	0.0000	19.367	22.6418	24.2704	0.4223
14 February 2025	0 [a]	0.00013 [a]	0 [a]	40.2471 [b]	0.0450	2.40838	9.80213	17.9749	0.4219
28 February 2025	0.447689 [a]	0.398657 [a]	4.66383 [a]	98.302 [b]	0.0000	28.5453	25.2224	24.0914	0.3280
14 March 2025	2.62442 [a]	6.22158 [a]	27.3509 [a]	99.971 [b]	0.0005	44.7762	29.0557	28.294	0.2609
28 March 2025	8.2702 [a]	8.97807 [a]	39.3158 [a]	90.543 [b]	0.0061	42.9647	38.4241	28.9415	0.6053
4 April 2025	5.03533 [a]	3.37268 [a]	55.9775 [b]	99.9362 [c]	0.0007	49.8008	41.4632	31.9773	0.3252
11 April 2025	97.4524 [b]	24.8552 [a]	78.5935 [b]	99.4975 [b]	0.0006	78.8062	77.6975	68.7953	0.4334
22 April 2025	99.3639 [b]	75.7128 [a]	97.9845 [b]	96.3394 [b]	0.0076	95.3773	91.4255	90.2477	0.4753
28 April 2025	99.217 [b]	87.2804 [a]	98.5573 [b]	99.9557 [b]	0.0691	97.9892	97.5044	93.2642	0.4200
5 May 2025	99.8733 [b]	89.9163 [a]	99.4275 [b]	99.9792 [b]	0.0724	98.1773	98.8445	94.8756	0.4297
12 May 2025	98.4159 [ab]	88.3818 [a]	89.2069 [ab]	99.7559 [b]	0.0839	96.971	94.4988	90.3505	0.2930
19 May 2025	92.5972	91.8002	91.7359	99.3103	0.4038	94.0939	96.2874	91.2014	0.5141
5 June 2025	89.5445	94.6713	90.0108	90.439	0.6795	80.0426 [a]	94.1265 [b]	99.3302 [b]	0.0072

Table A2. Average values and assigned groups for multifactorial ANOVA for different dates using adapted greenness index values. Different lowercase letters indicate significant differences (LSD test, $p < 0.05$).

Date	C	Z	R	T	*p*-Value	S1	S2	S3	*p*-Value
31 January 2025	0.165095 [a]	0.418733 [b]	0.435819 [b]	0.931378 [c]	0.0000	0.521749	0.409425	0.448537	0.8752
14 February 2025	0.199528 [a]	0.410594 [b]	0.520651 [c]	0.97828 [d]	0.0000	0.576863	0.536898	0.468029	0.0504
28 February 2025	0.142072 [a]	0.342335 [b]	0.368251 [b]	0.986956 [c]	0.0000	0.521749	0.409425	0.448537	0.1533
14 March 2025	0.357771 [a]	0.582361 [b]	0.590951 [b]	0.996797 [c]	0.0008	0.650761	0.722823	0.522325	0.0527
28 March 2025	0.924572 [a]	0.979052 [ab]	0.920121 [a]	0.999165 [b]	0.0444	0.966886	0.964438	0.935858	0.3429
4 April 2025	0.780347	0.870193	0.857546	0.997943	0.0560	0.923846 [b]	0.950876 [b]	0.7548 [a]	0.0186
11 April 2025	0.905426 [ab]	0.837879 [a]	0.925137 [ab]	0.993311 [b]	0.0274	0.955222	0.919517	0.871575	0.0926
22 April 2025	0.897241	0.953549	0.97622	0.983295	0.0635	0.94663	0.950952	0.960146	0.8429
28 April 2025	0.999188 [b]	0.997944 [ab]	0.995086 [a]	0.99967 [b]	0.0429	0.998328	0.998201	0.997387	0.6740
5 May 2025	0.760772	0.978102	0.985657	0.997848	0.2168	0.844255	0.971455	0.976075	0.3769
12 May 2025	0.980085	0.956422	0.979042	0.995242	0.2716	0.992991	0.975004	0.965099	0.2540
19 May 2025	0.742733	0.891417	0.645526	0.910489	0.0277	0.792922 [ab]	0.887146 [b]	0.712556 [a]	0.0767
5 June 2025	0.79483 [a]	0.925982 [b]	0.879433 [b]	0.948546 [b]	0.0087	0.850188	0.902381	0.909023	0.1187

Table A3. Average values and assigned groups for multifactorial ANOVA for different dates using adapted homogeneity index values. Different lowercase letters indicate significant differences (LSD test, $p < 0.05$).

Date	C	Z	R	T	*p*-Value	S1	S2	S3	*p*-Value
31 January 2025	−0.515907 ^{a}	0.00127343 ^{b}	0.150733 ^{b}	0.929484 ^{c}	0.0000	0.127986	0.133036	0.163165	0.8354
14 February 2025	−0.439512 ^{a}	−0.0101314 ^{b}	0.327393 ^{c}	0.98139 ^{d}	0.0000	0.301912	0.245509	0.0969337	0.0648
28 February 2025	−0.54168 ^{a}	−0.169054 ^{b}	−0.0074552 ^{b}	0.991234 ^{c}	0.0001	0.210785	−0.0377963	0.0317953	0.1360
14 March 2025	−0.059368 ^{a}	0.364342 ^{b}	0.430189 ^{b}	0.998821 ^{c}	0.0014	0.483625 ^{b}	0.603444 ^{b}	0.21342 ^{a}	0.0374
28 March 2025	0.903695	0.975678	0.885741	0.999006	0.0656	0.956363	0.957841	0.908886	0.3114
4 April 2025	0.735502	0.857682	0.817244	0.9975	0.0775	0.923493 ^{b}	0.94695 ^{b}	0.685503 ^{a}	0.0164
11 April 2025	0.939153	0.811151	0.910371	0.991927	0.0668	0.967378	0.919392	0.852681	0.1162
22 April 2025	0.951188	0.950502	0.981054	0.983201	0.2710	0.968574	0.959268	0.971616	0.7638
28 April 2025	0.99972	0.997585	0.994302	0.999986	0.1590	0.997617	0.997911	0.998167	0.9646
5 May 2025	0.662587	0.981412	0.98927	0.998929	0.4151	0.74815	0.986725	0.989273	0.4035
12 May 2025	0.986304	0.951509	0.983261	0.99756	0.3285	0.992832	0.982791	0.963352	0.3965
19 May 2025	0.662215 ^{b}	0.83795 ^{c}	0.435793 ^{a}	0.886607 ^{c}	0.0055	0.694806 ^{ab}	0.834948 ^{b}	0.587169 ^{a}	0.0326
5 June 2025	0.799143 ^{a}	0.92109 ^{b}	0.888252 ^{b}	0.943298 ^{b}	0.0292	0.832822	0.908318	0.922697	0.0579

Table A4. Average values and assigned groups for multifactorial ANOVA for different dates using GLI values. Different lowercase letters indicate significant differences (LSD test, $p < 0.05$).

Date	C	Z	R	T	*p*-Value	S1	S2	S3	*p*-Value
31 January 2025	0.0184556 ^{a}	0.0131889 ^{a}	0.0207111 ^{a}	0.0207111 ^{b}	0.0000	0.0575584	0.0543834	0.0492416	0.5203
14 February 2025	0.0188889 ^{a}	0.0158831 ^{a}	0.0198111 ^{a}	0.112955 ^{b}	0.0000	0.0464999	0.0382707	0.0408832	0.3742
28 February 2025	0.0211889 ^{a}	0.0374889 ^{a}	0.0317222 ^{a}	0.170811 ^{b}	0.0000	0.0796166 ^{b}	0.0622167 ^{ab}	0.054075 ^{a}	0.0459
14 March 2025	0.0743321 ^{a}	0.0811554 ^{a}	0.073211 ^{a}	0.213756 ^{b}	0.0000	0.130525 ^{b}	0.101799 ^{a}	0.0995166 ^{a}	0.0312
28 March 2025	0.0453444 ^{a}	0.0464778 ^{a}	0.0630445 ^{a}	0.122922 ^{b}	0.0002	0.0834333 ^{b}	0.0662418 ^{a}	0.0586667 ^{a}	0.0282
4 April 2025	0.0716778 ^{a}	0.0707 ^{a}	0.115255 ^{b}	0.193822 ^{c}	0.0000	0.12595 ^{b}	0.12125 ^{b}	0.0913916 ^{a}	0.0113
11 April 2025	0.142166 ^{b}	0.091 ^{a}	0.152756 ^{b}	0.235022 ^{c}	0.0001	0.167108	0.156158	0.142442	0.1349
22 April 2025	0.111945 ^{a}	0.131533 ^{a}	0.1735 ^{a}	0.238078 ^{b}	0.0102	0.171109	0.159642	0.160542	0.8484
28 April 2025	0.101678 ^{a}	0.112889 ^{a}	0.139333 ^{b}	0.178244 ^{c}	0.0016	0.142425	0.126883	0.1298	0.2817
5 May 2025	0.107622 ^{a}	0.165544 ^{b}	0.186745 ^{c}	0.244845 ^{d}	0.0000	0.166808	0.177442	0.184317	0.0679
12 May 2025	0.193178 ^{b}	0.168044 ^{a}	0.191322 ^{b}	0.237855 ^{c}	0.0018	0.197991	0.187241	0.207567	0.1192
19 May 2025	0.0928446 ^{a}	0.1544 ^{b}	0.143644 ^{b}	0.184711 ^{c}	0.0000	0.146033 ^{b}	0.132308 ^{a}	0.153358 ^{b}	0.0183
5 June 2025	0.1304 ^{ab}	0.168511 ^{a}	0.128633 ^{c}	0.151433 ^{bc}	0.0124	0.128475 ^{a}	0.146016 ^{ab}	0.159741 ^{b}	0.0194

References

1. Braun, R.C.; Mandal, P.; Nwachukwu, E.; Stanton, A. The role of turfgrasses in environmental protection and their benefits to humans: Thirty years later. *Crop Sci.* **2024**, *64*, 2909–2944. [CrossRef]
2. Trémeau, J.; Olascoaga, B.; Backman, L.; Karvinen, E.; Vekuri, H.; Kulmala, L. Lawns and meadows in urban green space—A comparison from perspectives of greenhouse gases, drought resilience and plant functional types. *Biogeosciences* **2024**, *21*, 949–972. [CrossRef]
3. Ignatieva, M.; Haase, D.; Dushkova, D.; Haase, A. Lawns in Cities: From a Globalised Urban Green Space Phenomenon to Sustainable Nature-Based Solutions. *Land* **2020**, *9*, 73. [CrossRef]
4. Monteiro, J.A. Ecosystem services from turfgrass landscapes. *Urban For. Urban Green.* **2017**, *26*, 151–157. [CrossRef]
5. Stier, J.C.; Steinke, K.; Ervin, E.H.; Higginson, F.R.; McMaugh, P.E. Turfgrass benefits and issues. *Turfgrass Biol. Use Manag.* **2013**, *56*, 105–145.
6. Hatfield, J. Turfgrass and climate change. *Agron. J.* **2017**, *109*, 1708–1718. [CrossRef]

7. Braun, R.C.; Straw, C.M.; Soldat, D.J.; Bekken, M.A.; Patton, A.J.; Lonsdorf, E.V.; Horgan, B.P. Strategies for reducing inputs and emissions in turfgrass systems. *Crop Forage Turfgrass Manag.* **2023**, *9*, e20218. [CrossRef]
8. Togawa-Urakoshi, Y.; Ueno, O. Photosynthetic nitrogen-and water-use efficiencies in C3 and C4 subtype grasses grown under two nitrogen supply levels. *Plant Prod. Sci.* **2022**, *25*, 183–194. [CrossRef]
9. Ozeki, K.; Miyazawa, Y.; Sugiura, D. Rapid stomatal closure contributes to higher water use efficiency in major C4 compared to C3 Poaceae crops. *Plant Physiol.* **2022**, *189*, 188–203. [CrossRef] [PubMed]
10. Baird, A.S.; Taylor, S.H.; Pasquet-Kok, J.; Vuong, C.; Zhang, Y.; Watcharamongkol, T.; Cochard, H.; Scoffoni, C.; Edwards, E.J.; Osborne, C.P.; et al. Resolving the contrasting leaf hydraulic adaptation of C3 and C4 grasses. *New Phytol.* **2025**, *245*, 1924–1939. [CrossRef]
11. Hejl, R.W.; Wherley, B.G.; Fontanier, C.H. Long-term Performance of Warm-season Turfgrass Species under Municipal Irrigation Frequency Restrictions. *HortScience* **2021**, *56*, 1221–1225. [CrossRef]
12. Trammell, T.L.; Pataki, D.E.; Still, C.J.; Ehleringer, J.R.; Avolio, M.L.; Bettez, N.; Cavender-Bares, J.; Groffman, P.M.; Grove, M.; Hall, S.J.; et al. Climate and lawn management interact to control C4 plant distribution in residential lawns across seven US cities. *Ecol. Appl.* **2019**, *29*, e01884. [CrossRef]
13. Pompeiano, A.; Grossi, N.; Guglielminetti, L.; Volterrani, M. Winter color retention and spring green-up of zoysiagrass genotypes in southern Europe. *Eur. J. Hortic. Sci.* **2014**, *79*, 158–166. [CrossRef]
14. Orta, A.H.; Todorovic, M.; Ahi, Y. Cool- and Warm-Season Turfgrass Irrigation with Subsurface Drip and Sprinkler Methods Using Different Water Management Strategies and Tools. *Water* **2023**, *15*, 272. [CrossRef]
15. Salama, A.-M.; Ezzat, A.; El-Ramady, H.; Alam-Eldein, S.M.; Okba, S.K.; Elmenofy, H.M.; Hassan, I.F.; Illés, A.; Holb, I.J. Temperate Fruit Trees under Climate Change: Challenges for Dormancy and Chilling Requirements in Warm Winter Regions. *Horticulturae* **2021**, *7*, 86. [CrossRef]
16. Fernandez, E.; Mojahid, H.; Fadón, E.; Rodrigo, J.; Ruiz, D.; Egea, J.A.; Ben Mimoun, M.; Kodad, O.; El Yaacoubi, A.; Ghrab, M.; et al. Climate change impacts on winter chill in Mediterranean temperate fruit orchards. *Reg. Environ. Change* **2023**, *23*, 7. [CrossRef]
17. Moon, M.; Seyednasrollah, B.; Richardson, A.D.; Friedl, M.A. Using time series of MODIS land surface phenology to model temperature and photoperiod controls on spring greenup in North American deciduous forests. *Remote Sens. Environ.* **2021**, *260*, 112466. [CrossRef]
18. Kim, A.-R.; Seol, J.; Lim, B.-S.; Lim, C.-H.; Kim, G.-S.; Lee, C.-S. Response of Plant Phenology on Microclimate Change Depending on Land Use Intensity in Seoul, Central Korea. *Forests* **2024**, *15*, 718. [CrossRef]
19. Uphus, L.; Uhler, J.; Tobisch, C.; Rojas-Botero, S.; Lüpke, M.; Benjamin, C.; Englmeier, J.; Fricke, U.; Ganuza, C.; Haensel, M.; et al. Earlier and more uniform spring green-up linked to lower insect richness and biomass in temperate forests. *Commun. Biol.* **2023**, *6*, 1052. [CrossRef]
20. Caturegli, L.; Lulli, F.; Foschi, L.; Guglielminetti, L.; Bonari, E.; Volterrani, M. Monitoring turfgrass species and cultivars by spectral reflectance. *Eur. J. Hortic. Sci.* **2014**, *79*, 97–107. [CrossRef]
21. Marín, J.; Yousfi, S.; Mauri, P.V.; Parra, L.; Lloret, J.; Masaguer, A. RGB Vegetation Indices, NDVI, and Biomass as Indicators to Evaluate C3 and C4 Turfgrass under Different Water Conditions. *Sustainability* **2020**, *12*, 2160. [CrossRef]
22. Yousfi, S.; Marín, J.; Parra, L.; Lloret, J.; Mauri, P.V. Remote sensing devices as key methods in the advanced turfgrass phenotyping under different water regimes. *Agric. Water Manag.* **2022**, *266*, 107581. [CrossRef]
23. Badzmierowski, M.J.; McCall, D.S.; Evanylo, G. Using Hyperspectral and Multispectral Indices to Detect Water Stress for an Urban Turfgrass System. *Agronomy* **2019**, *9*, 439. [CrossRef]
24. Bremer, D.J.; Lee, H.; Su, K.; Keeley, S.J. Relationships between Normalised Difference Vegetation Index and Visual Quality in Cool-Season Turfgrass: II. Factors Affecting NDVI and its Component Reflectances. *Crop Sci.* **2011**, *51*, 2219–2227. [CrossRef]
25. Ma, P.; Zhao, J.; Zhang, H.; Zhang, L.; Luo, T. Increased precipitation leads to earlier green-up and later senescence in Tibetan alpine grassland regardless of warming. *Sci. Total Environ.* **2023**, *871*, 162000. [CrossRef]
26. Cai, Y.; Sawada, K.; Makoto, K. How microclimate influences the spring phenological responses to decreased snow cover in four tree species seedlings in a boreal forest. *Sci. Rep.* **2025**, *15*, 10742. [CrossRef]
27. De Luca, V.; Gómez de Barreda, D. Effect of a Biostimulant on Bermudagrass Fall Color Retention and Spring Green-Up. *Agronomy* **2021**, *11*, 608. [CrossRef]
28. Çakır, M.; Mutlu, S.S.; Dönmez, Ş. Effects of Foliar Silicon and Nitrogen Applications on Winter Color Retention and Spring Green-Up of Zoysia Grass. *BioResources* **2024**, *19*, 8577–8593. [CrossRef]
29. Fu, Y.H.; Piao, S.; Zhao, H.; Jeong, S.; Wang, X.; Vitasse, Y.; Ciais, P.; Janssens, I.A. Unexpected role of winter precipitation in determining heat requirement for spring vegetation green-up at northern middle and high latitudes. *Glob. Change Biol.* **2014**, *20*, 3743–3755. [CrossRef]

30. Magni, S.; Gaetani, M.; Grossi, N.; Caturegli, L.; La Bella, S.; Leto, C.; Virga, G.; Tuttolomondo, T.; Lulli, F.; Volterrani, M. Bermudagrass adaptation in the Mediterranean climate: Phenotypic traits of 44 accessions. *Adv. Hortic. Sci. [Riv. Dell'ortoflorofrutticoltura Ital.]* **2014**, *28*, 29–34. [CrossRef]
31. Stewart, I.D.; Mills, G. *The Urban Heat Island*; Elsevier: Amsterdam, The Netherlands, 2021.
32. Al-Saadi, L.M.; Jaber, S.H.; Al-Jiboori, M.H. Variation of urban vegetation cover and its impact on minimum and maximum heat islands. *Urban Clim.* **2020**, *34*, 100707. [CrossRef]
33. Grover, A.; Singh, R.B. Analysis of urban heat island (UHI) in relation to normalized difference vegetation index (NDVI): A comparative study of Delhi and Mumbai. *Environments* **2015**, *2*, 125–138. [CrossRef]
34. Zipper, S.C.; Schatz, J.; Singh, A.; Kucharik, C.J.; Townsend, P.A.; Loheide, S.P. Urban heat island impacts on plant phenology: Intra-urban variability and response to land cover. *Environ. Res. Lett.* **2016**, *11*, 054023. [CrossRef]
35. Meng, L.; Mao, J.; Zhou, Y.; Richardson, A.D.; Lee, X.; Thornton, P.E.; Ricciuto, D.M.; Li, X.; Dai, Y.; Shi, X.; et al. Urban warming advances spring phenology but reduces the response of phenology to temperature in the conterminous United States. *Proc. Natl. Acad. Sci. USA* **2020**, *117*, 4228–4233. [CrossRef]
36. Kousis, I.; Pigliautile, I.; Pisello, A.L. Intra-urban microclimate investigation in urban heat island through a novel mobile monitoring system. *Sci. Rep.* **2021**, *11*, 9732. [CrossRef]
37. Yang, Y.; Qiu, X.; Yang, L.; Lee, D. Impacts of thermal differences in surfacing urban heat islands on vegetation phenology. *Remote Sens.* **2023**, *15*, 5133. [CrossRef]
38. MathWorks. *MATLAB*, Version R2025a; Computer Software; The MathWorks, Inc.: Natick, MA, USA, 2025. Available online: https://www.mathworks.com (accessed on 23 May 2026).
39. Mauri, P.V.; Marín, J.F.; Peña, J.M.; Muñoz, F.J.; Garcia de Paredes, M.P.; Centeno, A.; Parra, L. Evolution of Greenness and Uniformity of Grass Coverage of C4 Species During Spring Green-up Compared with a C3 Turfgrass. In *Proceedings of the First International Conference on Digitalization and Smart Solutions (DIGITAS 2025), Nice/Saint-Laurent-du-Var, France, 16–20 November 2025*; DTR Society: Nice/Saint-Laurent-du-Var, France, 2025.
40. Patrignani, A.; Ochsner, T.E. Canopeo: A powerful new tool for measuring fractional green canopy cover. *Agron. J.* **2015**, *107*, 2312–2320. [CrossRef]
41. Eng, L.S.; Ismail, R.; Hashim, W.; Baharum, A. The use of VARI, GLI, and VIgreen formulas in detecting vegetation in aerial images. *Int. J. Technol.* **2019**, *10*, 1385–1394. [CrossRef]
42. Barbosa, B.D.S.; Ferraz, G.A.S.; Gonçalves, L.M.; Marin, D.B.; Maciel, D.T.; Ferraz, P.F.P.; Rossi, G. RGB vegetation indices applied to grass monitoring: A qualitative analysis. *Agron. Res.* **2019**, *17*, 349–357.
43. Agapiou, A. Vegetation extraction using visible-bands from openly licensed unmanned aerial vehicle imagery. *Drones* **2020**, *4*, 27. [CrossRef]
44. Ashapure, A.; Jung, J.; Chang, A.; Oh, S.; Maeda, M.; Landivar, J. A comparative study of RGB and multispectral sensor-based cotton canopy cover modelling using multi-temporal UAS data. *Remote Sens.* **2019**, *11*, 2757. [CrossRef]
45. Statgraphics Technologies, Inc. *Statgraphics Centurion XVIII*, Version 18; Statgraphics Technologies, Inc.: The Plains, VA, USA, 2024.
46. Hardegree, S.P.; Sheley, R.L.; Duke, S.E.; James, J.J.; Boehm, A.R.; Flerchinger, G.N. Temporal variability in microclimatic conditions for grass germination and emergence in the sagebrush steppe. *Rangel. Ecol. Manag.* **2016**, *69*, 123–128. [CrossRef]
47. Boehm, A.R.; Hardegree, S.P.; Glenn, N.F.; Reeves, P.A.; Moffet, C.A.; Flerchinger, G.N. Slope and aspect effects on seedbed microclimate and germination timing of fall-planted seeds. *Rangel. Ecol. Manag.* **2021**, *75*, 58–67. [CrossRef]
48. Rossini, F.; Ruggeri, R.; Celli, T.; Rogai, F.M.; Kuzmanović, L.; Richardson, M.D. Cool-season grasses for overseeding sport turfs: Germination and performance under limiting environmental conditions. *HortScience* **2019**, *54*, 555–563. [CrossRef]
49. Ghaleb, W.; Ahmed, L.Q.; Wagner, M.H.; Eprinchard-Ciesla, A.; Olivares-Rodríguez, W.E.; Perrot, C.; Chenu, K.; Norton, M.; Escobar-Gutiérrez, A.J. The concepts of seed germination rate and germinability: A re-evaluation for cool-season grasses. *Agronomy* **2022**, *12*, 1291. [CrossRef]
50. Butler, T.J.; Celen, A.E.; Webb, S.L.; Krstic, D.B.; Interrante, S.M. Germination in cool-season forage grasses under a range of temperatures. *Crop Sci.* **2017**, *57*, 1725–1731. [CrossRef]
51. Esmaili, S.; Salehi, H. Effects of temperature and photoperiod on postponing bermudagrass (*Cynodon dactylon* [L.] Pers.) turf dormancy. *J. Plant Physiol.* **2012**, *169*, 851–858. [CrossRef]
52. Xie, L.J.; Zhu, H.S.; Guo, H.M.; Li, D.Y. Leaf structural and physiological factors for winter dormancy color of zoysiagrass (*Zoysia* spp. Willd.). *Eur. J. Hortic. Sci.* **2022**, *87*, 20220306117. [CrossRef]
53. Magni, S.; Pompeiano, A.; Volterrani, M. Zoysiagrass use and culture in Europe. *Int. Turfgrass Soc. Res. J.* **2017**, *13*, 44–47. [CrossRef]
54. Schiavon, M.; Leinauer, B.; Sevastionova, E.; Serena, M.; Maier, B. Warm-season turfgrass quality, spring green-up, and fall color retention under drip irrigation. *Appl. Turfgrass Sci.* **2011**, *8*, 1–9.
55. Hinton, J.D.; Livingston, D.P., III; Miller, G.L.; Peacock, C.H.; Tuong, T. Freeze tolerance of nine zoysiagrass cultivars using natural cold acclimation and freeze chambers. *HortScience* **2012**, *47*, 112–115. [CrossRef]

56. Patton, A.J.; Reicher, Z.J. Zoysiagrass species and genotypes differ in their winter injury and freeze tolerance. *Crop Sci.* **2007**, *47*, 1619–1627. [CrossRef]
57. Carr, T.Q.; Hutchens, W.J.; Patton, A.J.; Braun, R.C.; McFadden, D.; Richardson, M.D. Management strategies for preventing and recovering from zoysiagrass winterkill. *Crop Forage Turfgrass Manag.* **2025**, *11*, e70050. [CrossRef]
58. Wang, B.; Liu, Z.; Lu, J.; Cai, M.; Zhou, C.; Duan, G.; Yang, P.; Hu, J. An earlier spring phenology reduces vegetation growth rate during the green-up period in temperate forests. *Forests* **2023**, *14*, 1984. [CrossRef]
59. Li, Y.; Fan, S.; Li, K.; Zhang, Y.; Dong, L. Microclimate in an urban park and its influencing factors: A case study of Tiantan Park in Beijing, China. *Urban Ecosyst.* **2021**, *24*, 767–778. [CrossRef]
60. Yang, Y.; Cao, C.; Bogoev, I.; Deetman, C.; Dietz, G.; Hang, J.; Howard, L.; Huang, X.; Kendall, N.; Lai, J.; et al. Regulation of humid heat by urban green space across a climate wetness gradient. *Nat. Cities* **2024**, *1*, 871–879. [CrossRef]
61. Parece, T.E.; Campbell, J.B. Intra-urban microclimate effects on phenology. *Urban Sci.* **2018**, *2*, 26. [CrossRef]
62. Li, F.; Wu, C.; Chen, H.; Feng, X.; Li, M. Optimizing Urban Green Space Ecosystem Services for Climate Resilience: A Multi-Dimensional Assessment of Urban Park Cooling Effects. *Forests* **2026**, *17*, 383. [CrossRef]
63. Cosmulescu, S. Phenology of plants in urban environments and response to climate changes. A review. *SWJ Hortic. Biol. Environ.* **2023**, *14*, 57–75.
64. Weryszko-Chmielewska, E.; Piotrowska-Weryszko, K.; Dąbrowska, A. Response of Tilia sp. L. to climate warming in urban conditions–Phenological and aerobiological studies. *Urban For. Urban Green.* **2019**, *43*, 126369. [CrossRef]
65. Arellano, B.; Zheng, Q.; Roca, J. Analysis of climate change effects on precipitation and temperature trends in Spain. *Land* **2025**, *14*, 85. [CrossRef]
66. Bushenkova, A.; Soares, P.M.; Johannsen, F.; Lima, D.C. Towards an improved representation of the urban heat island effect: A multi-scale application of XGBoost for madrid. *Urban Clim.* **2024**, *55*, 101982.
67. Kouklis, G.R.; Yiannakou, A. The contribution of urban morphology to the formation of the microclimate in compact urban cores: A study in the city center of Thessaloniki. *Urban Sci.* **2021**, *5*, 37. [CrossRef]
68. Jiang, N.; Shen, M.; Yang, Z. Differential phenological responses to temperature among various stages of spring vegetation green-up. *J. Plant Ecol.* **2024**, *17*, rtae063. [CrossRef]
69. Liu, Y.; Zhang, Y.; Peñuelas, J.; Kannenberg, S.A.; Gong, H.; Yuan, W.; Wu, C.; Zhou, S.; Piao, S. Drought legacies delay spring green-up in northern ecosystems. *Nat. Clim. Change* **2025**, *15*, 444–451. [CrossRef]
70. Post, A.K.; Hufkens, K.; Richardson, A.D. Predicting spring green-up across diverse North American grasslands. *Agric. For. Meteorol.* **2022**, *327*, 109204. [CrossRef]
71. Tao, Z.; Huang, W.; Wang, H. Soil moisture outweighs temperature for triggering the green-up date in temperate grasslands. *Theor. Appl. Climatol.* **2020**, *140*, 1093–1105. [CrossRef]

Disclaimer/Publisher's Note: The statements, opinions and data contained in all publications are solely those of the individual author(s) and contributor(s) and not of MDPI and/or the editor(s). MDPI and/or the editor(s) disclaim responsibility for any injury to people or property resulting from any ideas, methods, instructions or products referred to in the content.